25 cy

THE OHIO STATE UNIVERSITY

RESEARCH FOUNDATION

1314 KINNEAR ROAD COLUMBUS, OHIO 43212

Report No. COO-2018-21 (Q-6)

STRESS CORROSION CRACKING OF Fe-Cr-Ni ALLOYS IN CAUSTIC ENVIRONMENTS

A. K. Agrawal and R. W. Staehle
Department of Metallurgical Engineering

April 15, 1970 - July 14, 1970

U. S. Atomic Energy Commission
Chicago Operations Office
Argonne, Illinois

Contract No. AT(11-1)-2018

DISCLAIMER

LEGAL NOTICE

DISTRIBUTION LIST

	Copies
U. S. Atomic Energy Commission Division of Reactor Development & Technology Washington, D.C. 20545	
Attn: Director	1
Special Assistant to the Director	1
Assistant Director for Project Management	1
Assistant Director for Plant Engineering	1
Assistant Director for Reactor Engineering	1
Assistant Director for Reactor Technology	1
Assistant Director for Program Analysis	1
Assistant Director for Engineering Standards	1
Chief, Coolant Chemistry Branch	3
Chief, Fuels and Materials Branch	1
Chief, Reactor Vessels Branch	1
Chief, Liquid Metal Projects Branch	1
Chief, Fuel Engineering Branch	1
Chief, Liquid Metal Systems Branch	1
LMFBR Program Manager	1
Assistant Director, RDT, Pacific Northwest Programs U. S. Atomic Energy Commission P. O. Box 550 Richland, Washington 99352	1
Assistant Director for Reactor Technology Division of Reactor Licensing U. S. Atomic Energy Commission (Bethesda - 010) Washington, D.C. 20545	2
Director Division of Reactor Standards U. S. Atomic Energy Commission (Bethesda - 010) Washington, D.C. 20545	2
U. S. Atomic Energy Commission Librarian Washington, D.C. 20545	2
RDT Site Office U. S. Atomic Energy Commission Idaho Operations Office P. O. Box 2108 Idaho Falls, Idaho 83401	1

	Copies
RDT Site Office U. S. Atomic Energy Commission Argonne National Laboratory 9700 South Cass Avenue Argonne, Illinois 60439	1
RDT Site Office U. S. Atomic Energy Commission P. O. Box 1446 Canoga Park, California 91304	1
RDT Site Office U. S. Atomic Energy Commission 310 DeGuigne Drive Sunnyvale, California 94086	1
RDT Site Office Oak Ridge National Laboratory U. S. Atomic Energy Commission P. O. Box X Oak Ridge, Tennessee 37830	1
RDT Site Office U. S. Atomic Energy Commission Westinghouse Electric Corporation P. O. Box 154 Madison, Pennsylvania 15663	1
RDT Site Office Gulf General Atomic U. S. Atomic Energy Commission P. O. Box 2325 San Diego, California 92112	1
President Hanford Engineering Development Laboratory P. O. Box 1970 Richland, Washington 99352	1
Project Manager, FFTF Hanford Engineering Development Laboratory P. O. Box 1970 Richland, Washington 99352	5
Director LMFBR Program Office Argonne National Laboratory 9700 South Cass Avenue Argonne, Illinois 60439	4

	Copies
Associate Director Engineering Research and Development Argonne National Laboratory 9700 South Cass Avenue Argonne, Illinois 60439	5
Associate Director for Reactor and Engineering Sciences Oak Ridge National Laboratory P. O. Box X Oak Ridge, Tennessee 37830	1
Director Liquid Metal Engineering Center Atomics International Division of North American Aviation, Inc. P. O. Box 309 Canoga Park, California 91305	5
Manager Idaho Nuclear Corporation Research and Development Department Atomic Energy Division P. O. Box 1845 Idaho Falls, Idaho 83401	1
Head Metallurgy and Materials Science Division Department of Applied Science Brookhaven National Laboratory Associated Universities, Inc. Upton, L. I., New York 11973	
Foster Wheeler Corporation 110 South Orange Avenue Livingston, New Jersey 07039	1
Mine Safety Corporation Division of Mine Safety Appliances Company Evans City, Pennsylvania 16033	1
Byron Jackson Pump Division P. O. Box 2017 Los Angeles, California 90045	1
Office of the President Atomics International A Division of North American Rockwell Corporation P. O. Box 309 Canoga Park, California 91304	1

	Copies
Chief Project Manager Fast Reactor Components Power Generation Division Babcock and Wilcox Company Barberton, Ohio 44203	1
Babcock and Wilcox Company Atomic Energy Division P. O. Box 1260 1201 Kemper Street Lynchburg, Virginia 24505	2
Associate Manager Materials Engineering Department Battelle Memorial Institute Columbus Laboratory 505 King Avenue Columbus, Ohio 43201	1
Combustion Engineering, Inc. Office of the Vice President Nuclear Power Department P. O. Box 500 Windsor, Connecticut 06095	2
Manager, Advanced Reactor Division Westinghouse Electric Corporation P. O. Box 355 Pittsburgh, Pennsylvania 15230	3
Office of the Vice President Atomic Power Development Associates, Inc. 1911 First Street Detroit, Michigan 48226	1
Gulf-General Atomic, Inc. Librarian P. O. Box 608 San Diego, California 92112	1
General Manager Breeder Reactor Development Operation General Electric Company 310 DeGuigne Drive Sunnyvale, California 94086	3
Manager, Research United Nuclear Corporation 5 New Street White Plains, New York 10601	1

	Copies
Nuclear Materials and Equipment Corporation P. O. Box 266 Apollo, Pennsylvania 15613	1
Division of Technical Information Extension Oak Ridge National Laboratory P. O. Box X Oak Ridge, Tennessee 37380	20
National Technical Information Service 5285 Port Royal Road Springfield, Virginia 22151	25
Director Contracts Division Atomic Energy Commission 9800 Cass Avenue Argonne, Illinois 60439	1

RF Project 2765

Report No. COO-2018-21

QUARTERLY

REPORT

By

THE OHIO STATE UNIVERSITY
RESEARCH FOUNDATION

1314 KINNEAR RD.
COLUMBUS, OHIO 43212

To U. S. ATOMIC ENERGY COMMISSION
Chicago Operations Office
9800 South Cass Avenue
Argonne, Illinois 60439
Contract No. AT(11-1)-2018

On STRESS CORROSION CRACKING OF Fe-Cr-Ni ALLOYS IN CAUSTIC ENVIRONMENTS

For the period April 15, 1970 - July 14, 1970

Submitted by A. K. Agrawal and R. W. Staehle
Department of Metallurgical Engineering

Date March 5, 1971

TABLE OF CONTENTS

LIST OF FIGURES

LIST OF FIGURES (continued)

1.0 ABSTRACT

Results from stress corrosion and electrochemical studies are reported for Fe-Cr-Ni alloys exposed to NaOH-H_2O solutions at temperatures below 200°C. Sensitized 304 stainless steel, as compared to annealed 304 stainless steel is more prone to SCC, and is unsuitable for either anodic or cathodic protection. Principal cause of failure is intergranular cracking. Cathodic polarization results show that hydrogen evolution on Fe-Cr-Ni alloys occur at approximately -1.1 V (SCE). Increase in temperature slightly shifts the hydrogen evolution potential to less negative values. Cathodic kinetics, relative to anodic kinetics, is independent of alloy composition, caustic concentration, and temperature.

2.0 CONCLUSIONS

1. Stress corrosion cracking of sensitized and vacuum annealed 304 stainless steel was investigated in boiling caustic solutions (20-80% NaOH) as a function of applied potentials. Cracking of sensitized specimens occurred in solutions of lower concentrations (30% NaOH) compared to that of annealed specimens (60% NaOH). Sensitized material failed mainly because of intergranular cracking, whereas, in the case of annealed material the principal cause was transgranular cracking. Corrosion potentials were lowered with sensitization, and an increase in anodic dissolution kinetics was observed. Possible reasons for such behaviors are, a) increased anodic character of chromium carbide enriched grain boundaries resulting from sensitization; b) decreased resistance of alloy due to depletion of Cr from grain boundaries; and c) mechanical disintegration of chromium carbide from grain boundaries.

2. Cathodic polarization studies of Fe-Cr-Ni alloys in 1 to 10N NaOH over 25-90°C temperature show that, in almost all instances, reduction of surface oxides is complete and hydrogen evolution occurs at approximately -1.1 V (SCE). The hydrogen evolution potential becomes slightly less negative with increase in temperature. In general, effect of alloy composition, caustic concentration, and temperature on hydrogen evolution kinetics is slight. Addition of Ni to alloys slowed the kinetics while temperature and caustic concentration accelerated it.

3. Design of an apparatus and experimental procedure to study stress corrosion cracking of alloys in fused NaOH environment are presented.

3.0 INTRODUCTION

This work is being conducted in support of the LMFBR activities to identify the possible incidences and extent of caustic stress corrosion cracking which could cause premature equipment failure. The most likely sites where such SCC is possible are (1) in the steam generator at the Na-H_2O interface and (2) on exterior surfaces where Na spills or leaks can hydrolyze to form NaOH solutions in the presence of moisture.

Caustic SCC is a serious consideration in iron base alloy systems and becomes generally more serious with increasing iron concentrations in the alloy as shown in COO-2018-4.

This program is approaching the problem by conducting both direct SCC studies and fundamental studies aimed at understanding the phenomenon. The work is outlined in a series of tasks. Work performed on a given task is described. Note that work is not performed each quarter on all tasks owing to schedule for starting the respective task and also to vagaries in academic schedules for graduate students.

4.0 PROGRESS IN INDIVIDUAL TASKS

Task 1 - Tests of Engineering Geometries

A. Aims

The purpose of this work is to conduct experiments which simulate possible failure modes in engineering geometries for the purpose of finding what kind of corrosion phenomena might occur in the event of a sodium leak. From this information more specific definitions could be given to fundamental studies.

B. Results

None this Quarter.

Task 2 - General Effects of Alloy and Environmental Composition in Aqueous Solvents on Stress Corrosion Cracking (D. V. Subrahmanyam)

A. Aims

The purpose of this task is to assess the general effects of environment and alloy chemistry on the incidence of caustic stress

corrosion cracking. Variables will include alloy chemistry, temperature, concentration of OH^-, identity of cation, dissolved gases including oxygen, and electrochemical potential.

B. Results

1. Introduction

Susceptibility to stress corrosion cracking can be significantly altered by a change in the heat treatment procedure. Sensitization is one of such influential heat treatment parameters.

The effects of sensitization of 304 stainless steel has been studied in nitric acid containing sodium chloride,[1] in dilute chloride between 80-100°C temperature range,[2] and in nuclear and superheat environments.[1] The results were dependent on the environments used. In this report, the behavior of caustic cracking of sensitized stainless steel is compared with vacuum annealed stainless steel.

2. Experimental

a. Sensitization. Wires of 304 stainless steel, 15 ml diameter, were sealed in quartz capsules under argon atmosphere. These capsules were held at 1000°F for 10 hours and then air cooled.

b. Annealing. Procedure as in (a) was adopted at a temperature of 2200°F.

Specimen loading and other experimental details were described in previous reports.[3] The experiments involved the determination of failure times, crack morphologies, potential-time, and current-time behavior (under potentiostatic conditions) for sensitized and vacuum annealed specimens, as a function of NaOH concentration in the range 20-80% NaOH.

3. Results

a. Effect of NaOH concentration on failure times and crack morphologies. Figure 1 shows the effect of sensitization on failure times of 304 stainless steel at different NaOH concentrations. It can be seen that rapid failures occurred in case of sensitized specimens. Minimum NaOH concentration required to produce cracking was 50% for vacuum annealed specimens and 30% for sensitized specimens. Sensitization lowered the limiting concentration of NaOH to produce cracking.

The effect of NaOH concentration on crack morphologies of sensitized and vacuum annealed 304 stainless steel are shown in Fig. 2. The significant features in this figure are:

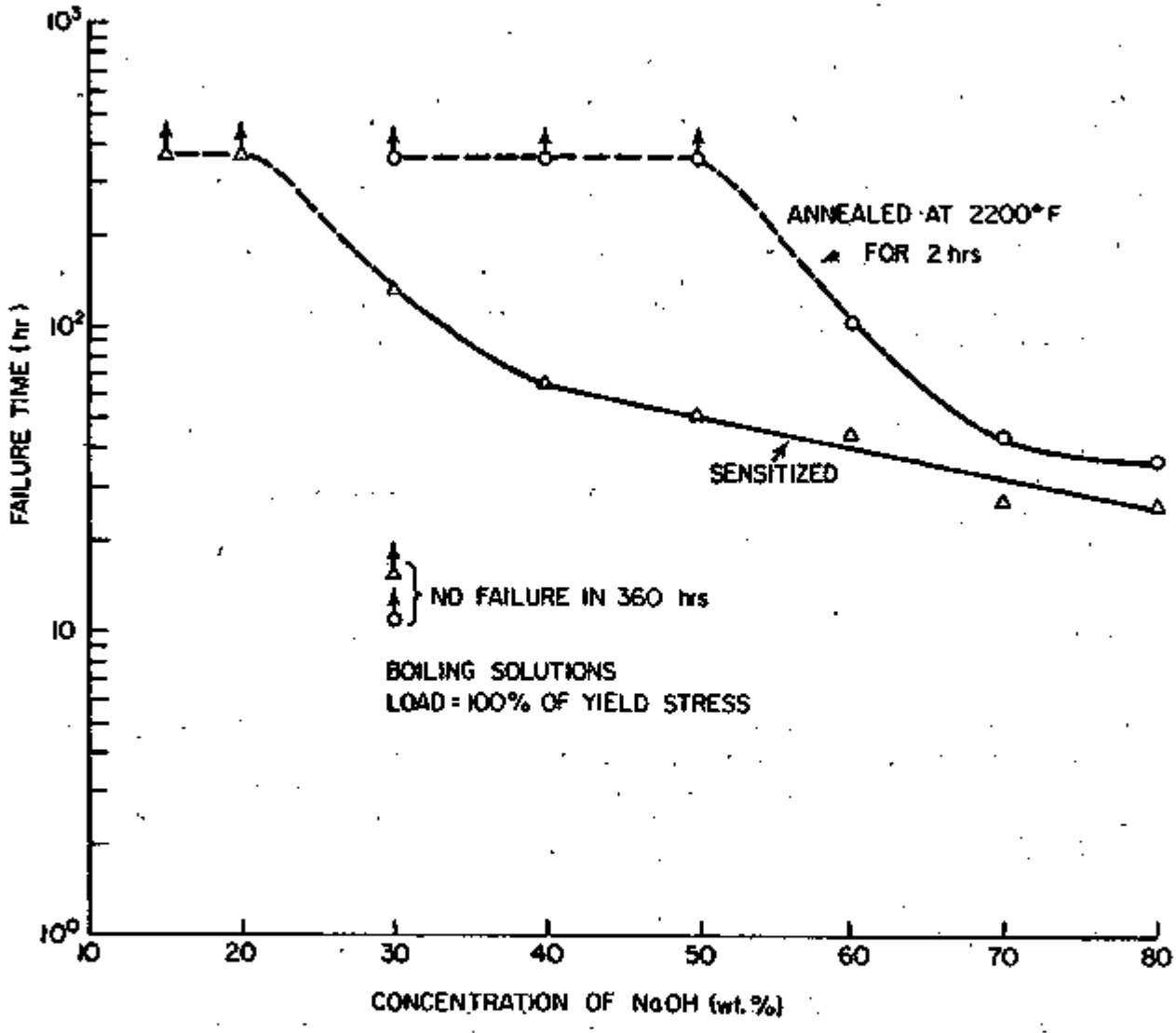

Fig. 1 - Effect of Sodium Hydroxide Concentration on Failure Times of Sensitized and Vacuum Annealed 304 Stainless Steel

80% NaOH

Sensitized

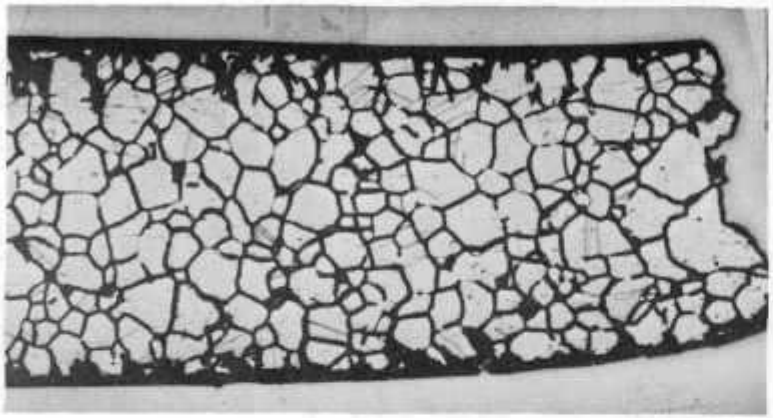

1. $E_{CORR} = -984mV_H$; T_f = 26.8 hr 150X

Vacuum-annealed

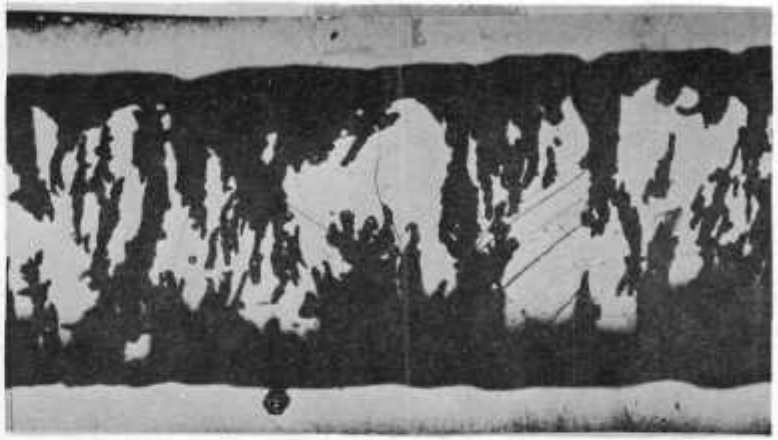

3. $E_{CORR} = -965mV_H$; T_f = 36 hr 150X

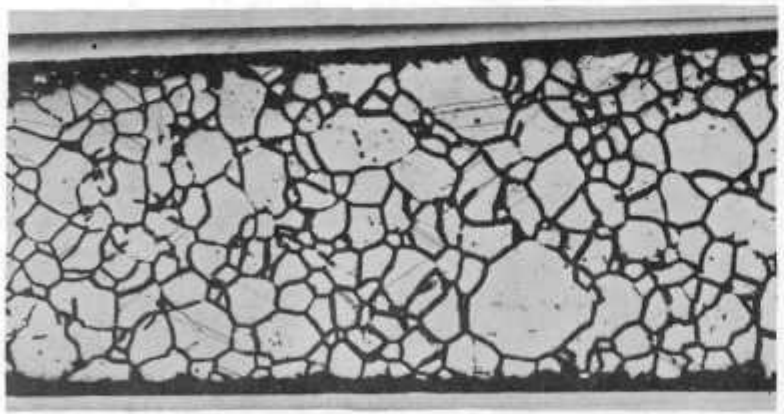

2. Unstressed, $E_{CORR} = -964mV_H$ 150X

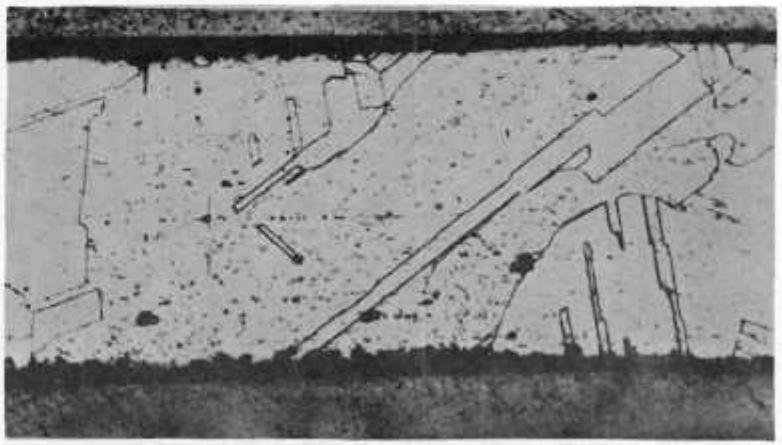

4. Unstressed, $E_{CORR} = -965mV_H$ 150X

Figure 2 - Effect of Sodium Hydroxide Concentration on Crack Morphologies of Sensitized and Annealed 304 Stainless Steel (Load = 100% of Y.S.)

60% NaOH

Sensitized

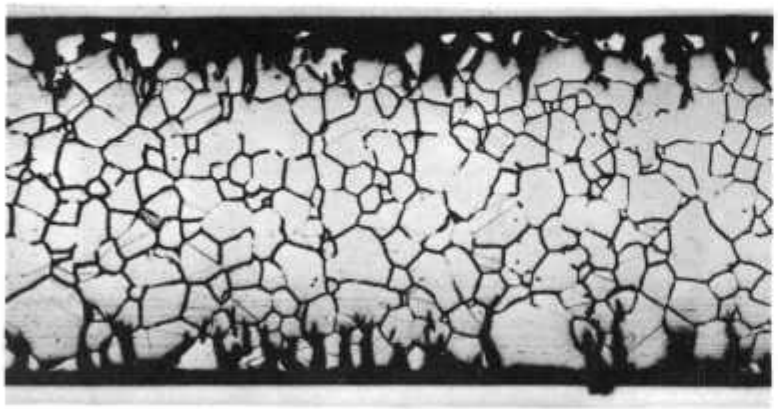

5. E_{CORR} = -914mV$_H$; T_f = 46 hr 150X

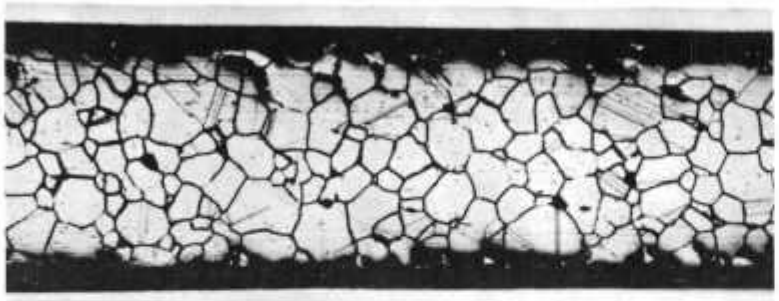

6. Unstressed; E_{CORR} = -979mV$_H$ 150X

Vacuum-annealed

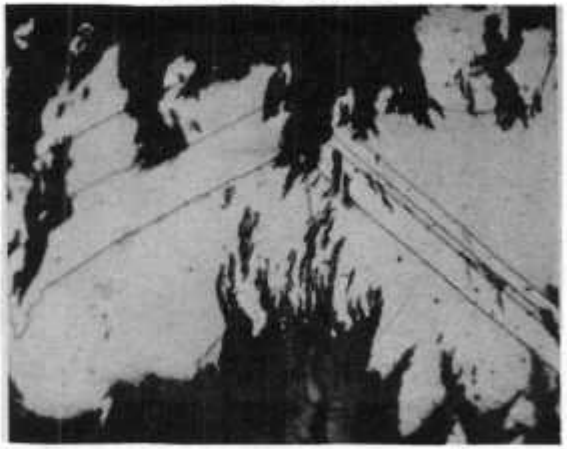

7. E_{CORR} = -942mV$_H$; T_f = 102 hr 150X

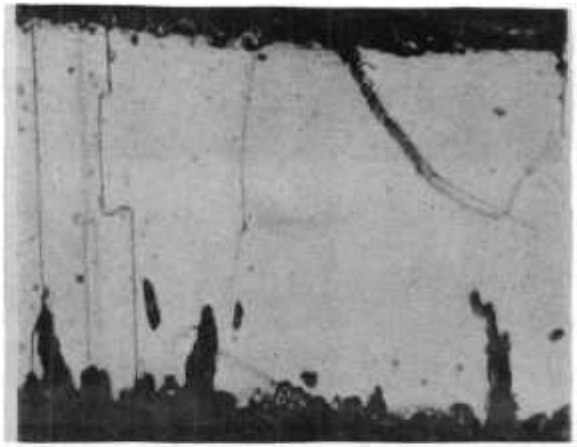

8. Unstressed; E_{CORR} = -935mV$_H$ 200X

Figure 2 - Continued

50% NaOH

Sensitized

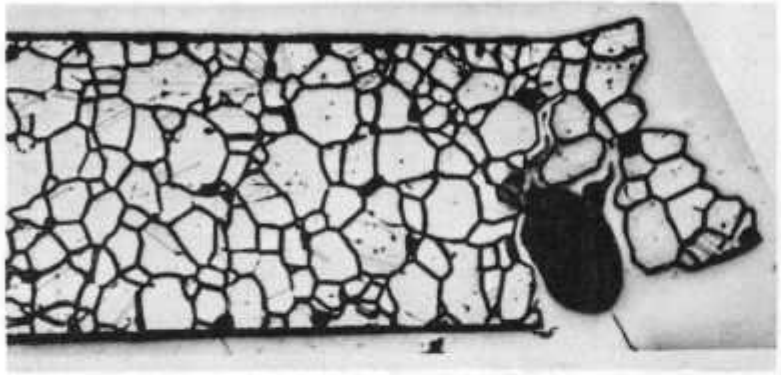

9. E_{CORR} = -894mV$_H$; T_f = 50.5 hr 150X

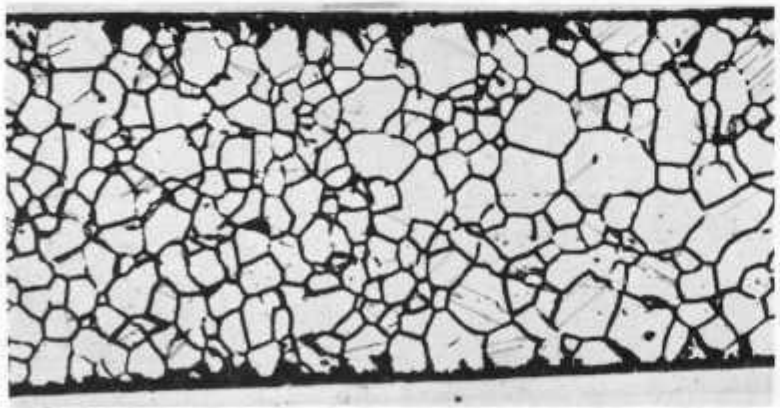

10. Unstressed; E_{CORR} = -909mV$_H$ 150X

Vacuum-annealed

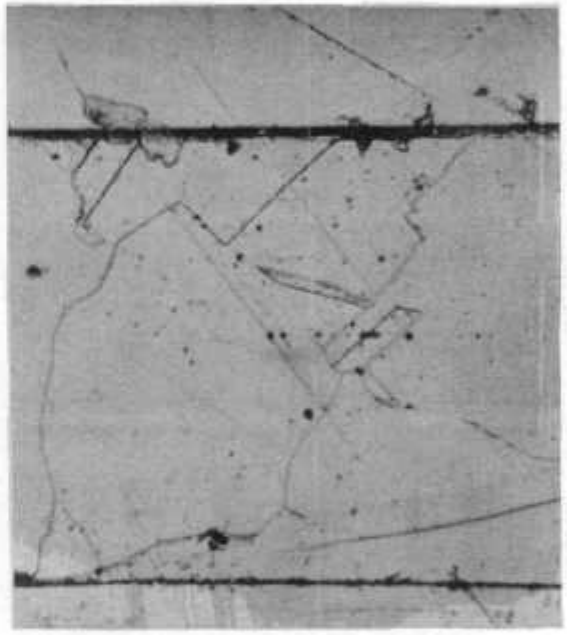

11. E_{CORR} = -369mV$_H$; T_f = No failure in 15 days 200X

Figure 2 - Continued

Sensitized

40% NaOH

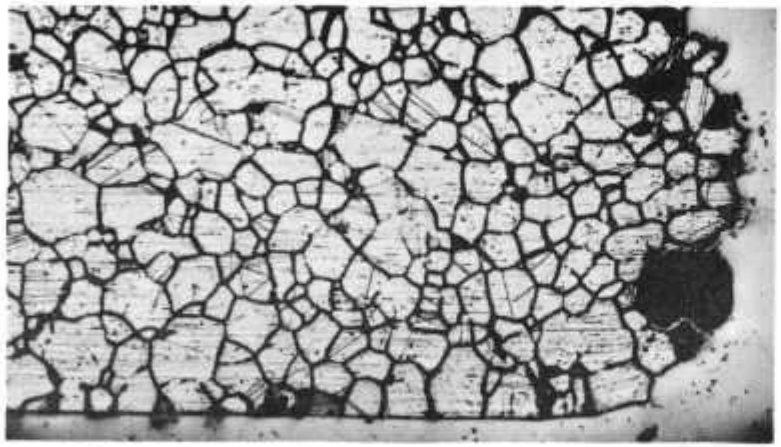

12. $E_{CORR} = -274mV_H$; T_f = 66 hr 150X

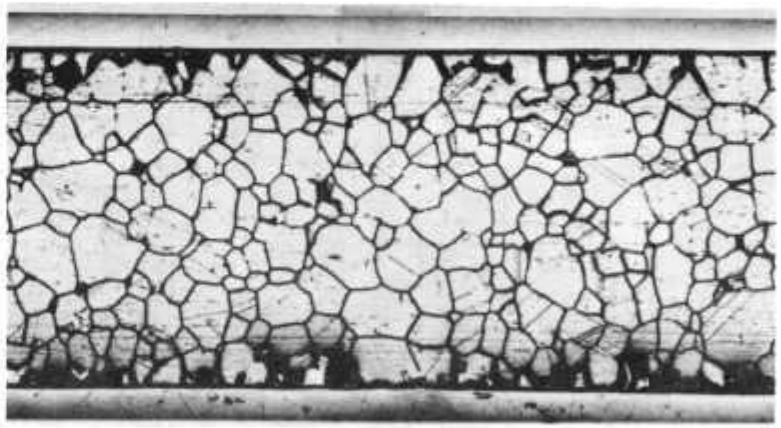

14. Unstressed; $E_{CORR} = -854mV_H$ 150X

30% NaOH

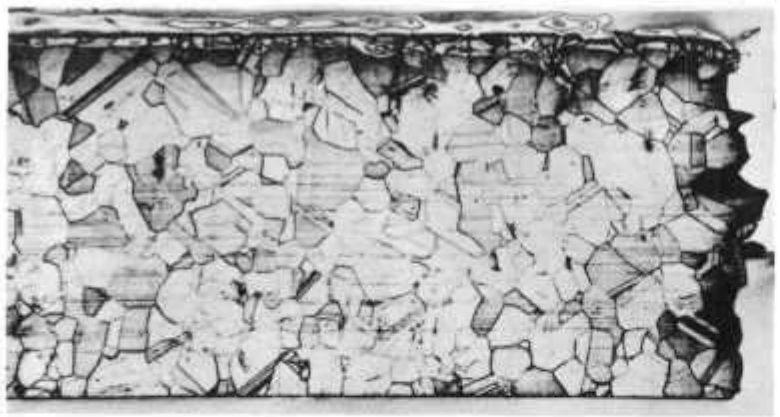

13. $E_{CORR} = -174mV_H$; T_f = 137 hr 150X

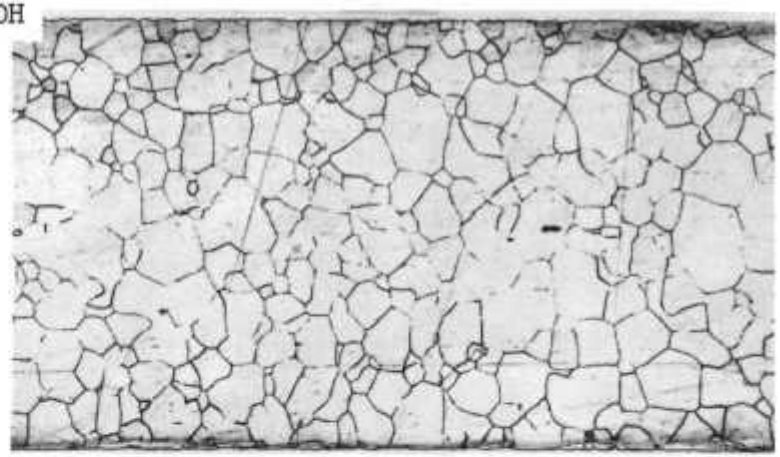

15. Unstressed; $E_{CORR} = -744mV_H$ 150X

Figure 2 - Continued

Sensitized
20% NaOH

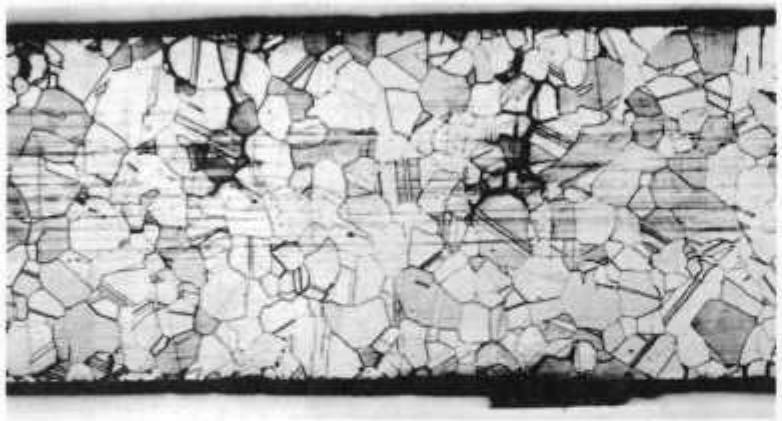

16. E_{CORR} = -4mV$_H$; T_f = 15 days (Not failed) 150X

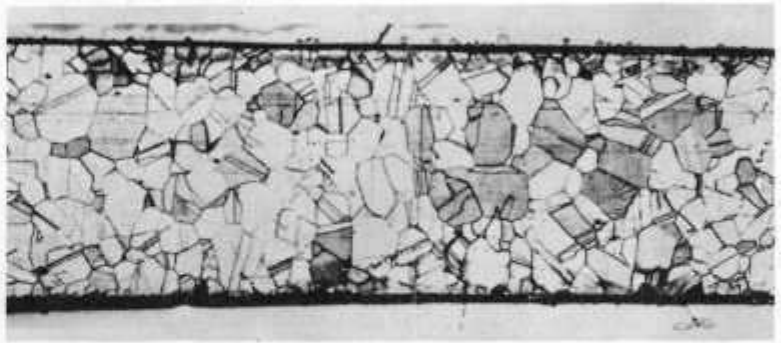

17. Unstressed; E_{CORR} = -164mV$_H$ 150X

Figure 2 - Continued

(i) Stressed and sensitized 304 stainless steel showed intergramular cracking at all concentrations with a negligible transgranular character (photos 1, 5, 9, 12, 13, and 16). The unstressed specimens exhibited intergramular corrosion (photos 2, 6, 10, 14, 15, and 17).

(ii) Vacuum annealed 304 stainless steel exhibited mixed type of cracks in 80% and 60% NaOH with a predominant transgranular character (photos 5 and 7). The specimen which did not fail in 50% NaOH showed a negligible amount of grain boundary attack (photo 11). The unstressed specimens in 80% and 60% NaOH showed generalized type of attack (photos 4 and 8). This was less severe than intergranular attack of sensitized specimen under unstressed conditions.

b. Effect of NaOH concentration on corrosion potentials and potential-time behavior. The effect of NaOH concentration on corrosion potentials of sensitized and vacuum annealed 304 stainless steel specimens is shown in Fig. 3. The sensitized specimens exhibited more negative corrosion potentials than vacuum annealed specimens. The effect of stressing was more pronounced at concentrations below 60% NaOH. The potential shifts were toward less negative values for sensitized samples, while it was toward negative values for vacuum annealed specimens.

The potential-time curves for 304 stainless steel in 70% NaOH solution are shown in Fig. 4. From these curves it can be seen that the corrosion potentials became more negative with time, for both sensitized and annealed specimens. This indicates that the dissolution kinetics is favored with time. It can also be noted that the steady state corrosion potential for sensitized specimens (-933 mV_H) are almost the same as that for vacuum annealed specimens (-924 mV_H).

(i) Potentiostatic polarization curves, cracking behavior and crack morphologies. The potentiostatic polarization curves for sensitized and vacuum annealed 304 stainless steel are shown in Fig. 5. The values of anodic and cathodic currents are summarized in Table I.

It can be seen that for the unstressed sensitized specimens anodic peak currents are higher by one order of magnitude. The cathodic and transpassive regions showed no significant effects of sensitization. Stressing had more effect on the sensitized specimens in cathodic regions, shifting the currents by almost two orders of magnitude.

The effect of potential on failure times in 70% boiling NaOH is shown in Fig. 6. Sensitized specimens failed earlier than vacuum annealed specimens. The potential did not have any significant effect on the failure times of sensitized specimens. It can also be observed that the cathodic protection is less applicable for sensitized materials.

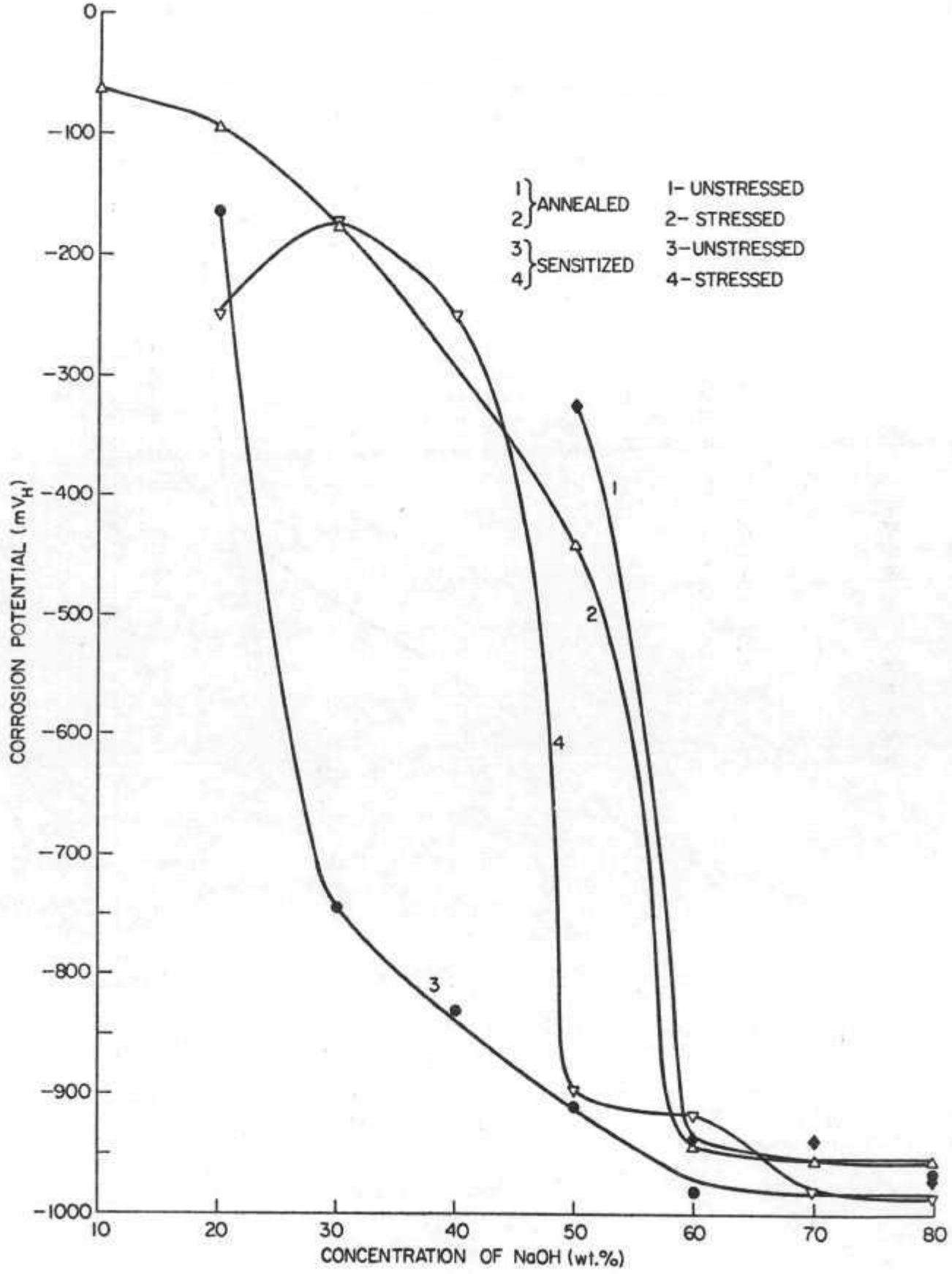

Fig. 3 - Effect of Sodium Hydroxide Concentration on Corrosion Potentials of Sensitized and Vacuum Annealed 304 Stainless Steel

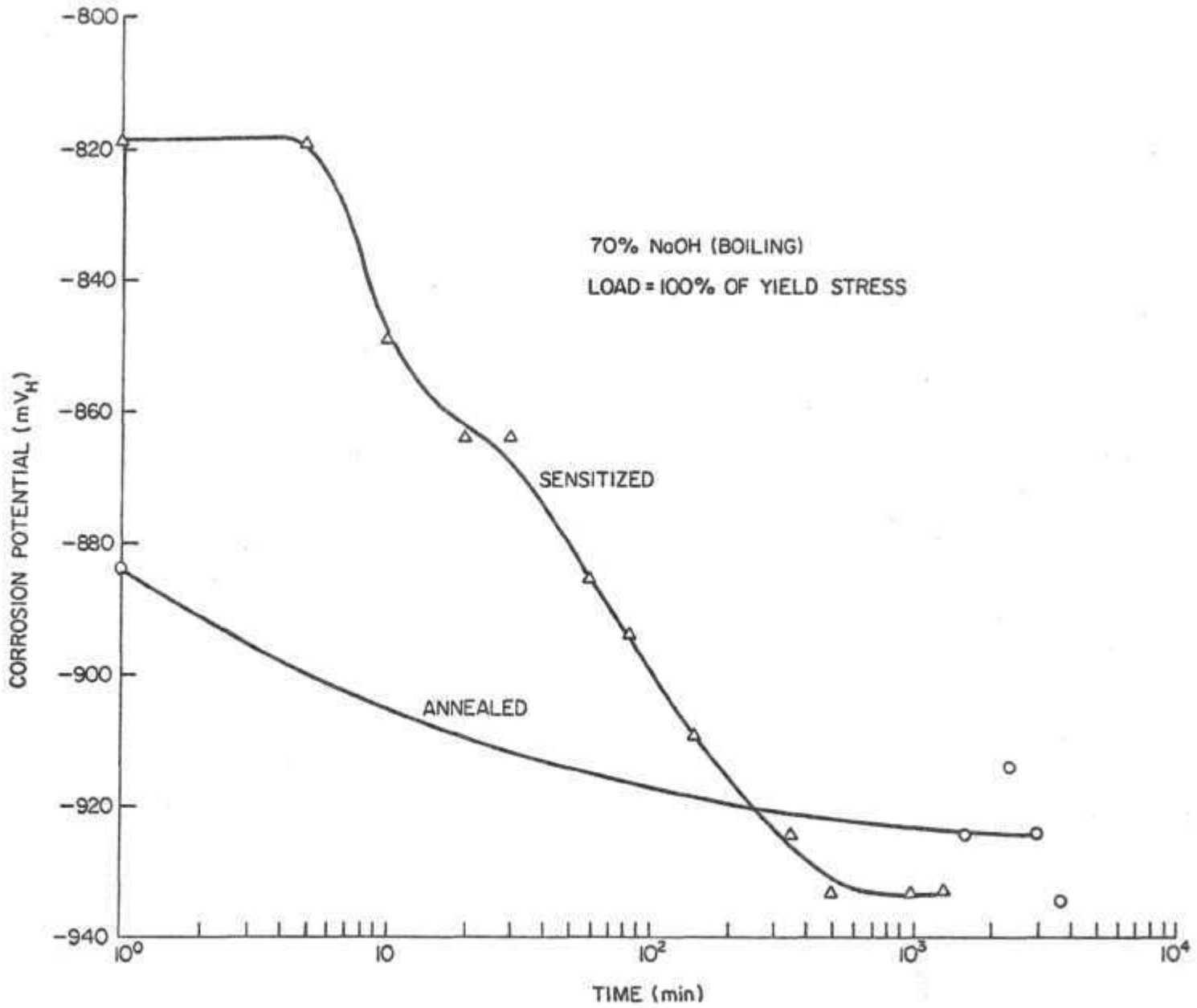

Fig. 4 - Potential-Time Curves for 304 Stainless Steel

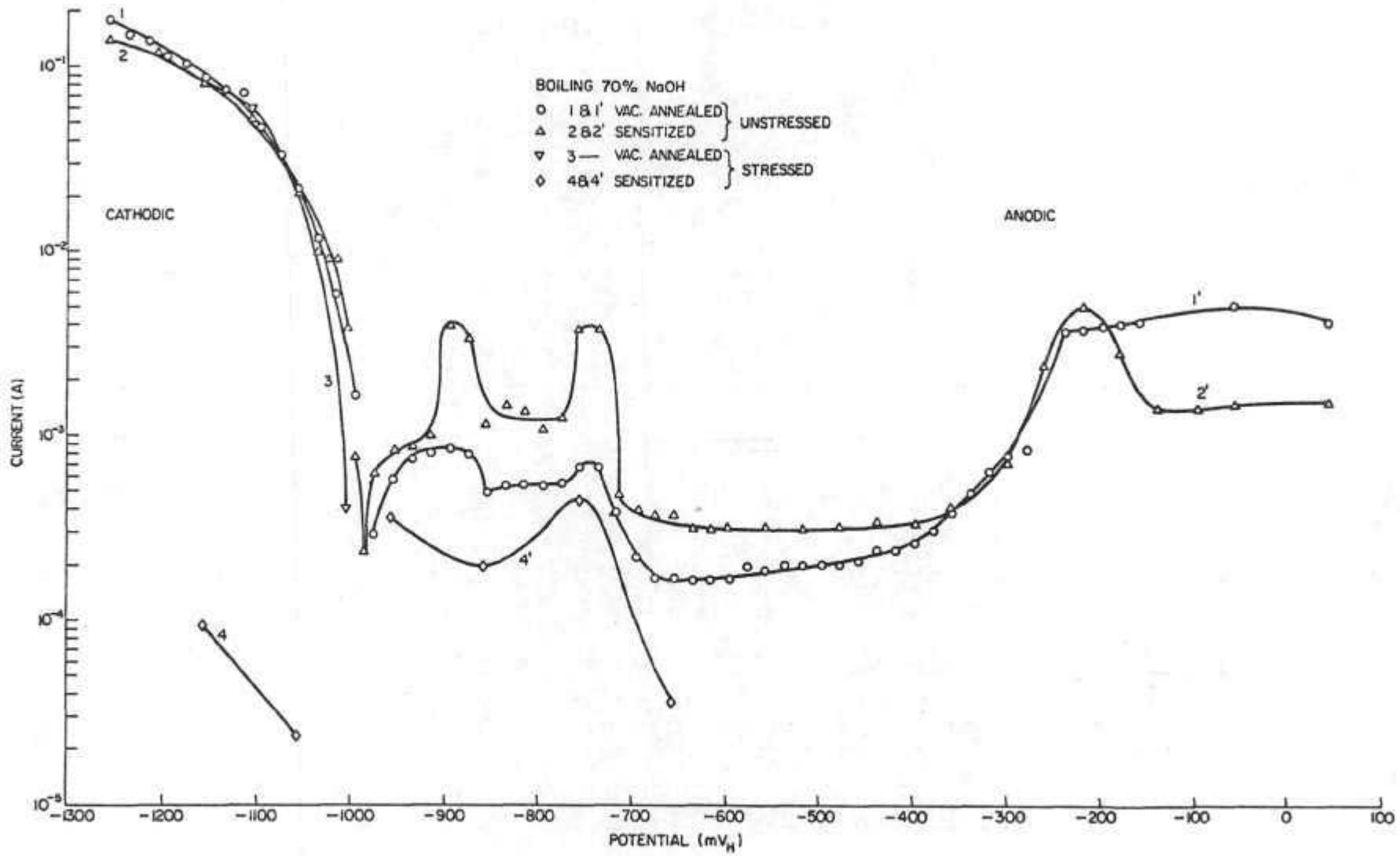

Fig. 5 - Effect of Sensitization on Potentiostat Behavior of 304 Stainless Steel

Table I - Values of Cathodic and Anodic Currents for Annealed and Sensitized 304 Stainless Steel in Boiling 70% NaOH

Condition	Current, A				
	Cathodic	Anodic			
		#1 Peak	#2 Peak	Passive	Transpassive
Vacuum Annealed Unstressed-Curves 1&1'	1.8×10^{-1} -- 1.7×10^{-3}	9×10^{-4}	7.2×10^{-4}	1.8 to 3.3×10^{-4}	2.6 to 3.6×10^{-3}
Sensitized-Curves Unstressed 2&2'	1.4×10^{-1} -- 4.0×10^{-3}	4.0×10^{-3}	4.0×10^{-3}	4.8 to 2.6×10^{-4}	5.0 to 1.5×10^{-3}
Vacuum Annealed Stressed-Curve 3	8.2×10^{-2} -- 4.2×10^{-4}				
Sensitized Stressed-Curves 4&4'	9.5 to 2.5×10^{-5}		4.6×10^{-4}		

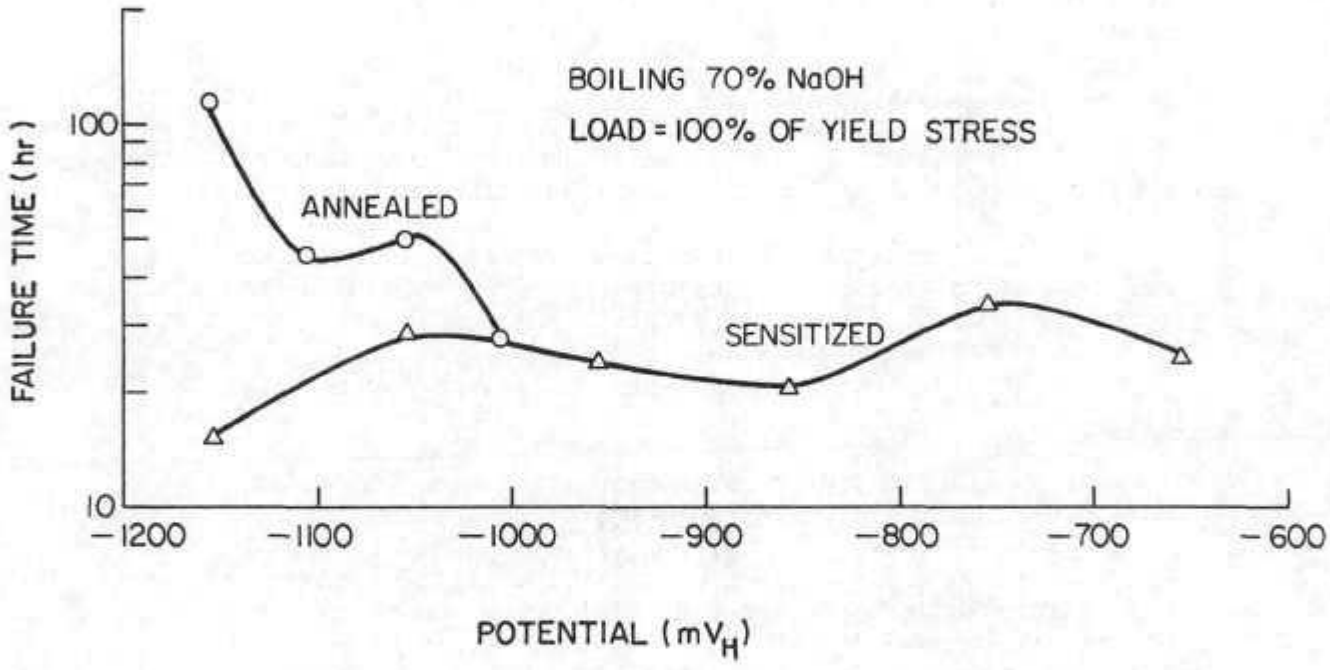

Fig. 6 - Effect of Potential on Failure Times of 304 Stainless Steel

The effect of potential on crack morphologies is shown in Fig. 7. The observed morphological features are summarized as a function of potential in Table II. At cathodic potentials, there was a change from transgranular to intergranular mode of failure as a result of sensitization. The data is insufficient to draw any conclusions on the effect of anodic potentials.

(ii) Current-time curves. The current time curves at cathodic potentials are shown in Fig. 8. For sensitized specimens, the current decreased with time after 100 minutes; while the currents were almost independent of time for annealed specimens. The sudden drop in current indicates the relative ease of failure of cathodic protection for sensitized materials.

4. Discussion

Experimental evidence indicates that sensitized 304 stainless steel is a poor alloy for industrial use since

(i) Cracking of sensitized specimens occurred in solution of lower caustic concentration (30% NaOH) compared to that of vacuum annealed specimens (60% NaOH);

(ii) Corrosion potentials were lowered with sensitization;

(iii) Anodic polarization curves show increased anodic dissolution kinetics for sensitized specimen.

(iv) Rapid failure of sensitized specimens occurred and failure was almost independent of potential in the range of potentials studied. (Similar rapid intergranular failures have been reported in nitric acid and chloride, nuclear and superheat environments).[1,2]

The observed results can be explained in the following way. Sensitization involved the intergranular precipitation of chromium carbide (Cr_7C_3) along the grain boundaries. Also, there was a considerable reduction in the grain size, approximately by a factor of two. These facts are illustrated in the photomicrographs of sensitized and vacuum annealed specimens in Fig. 9. The resistance of the alloy was significantly lowered due to the depletion of chromium from the alloy. Grain-boundary enrichment of chromium carbide increased the anodic character, leading to rapid intergranular failure and more negative corrosion potentials, which caused the pronounced anodic peaks in the polarization curves.

In a recent publication, Cron, Payer and Staehle[4] showed that in solutions up to pH of 14, Cr_7C_3 dissolves according to the

70% NaOH

Sensitized

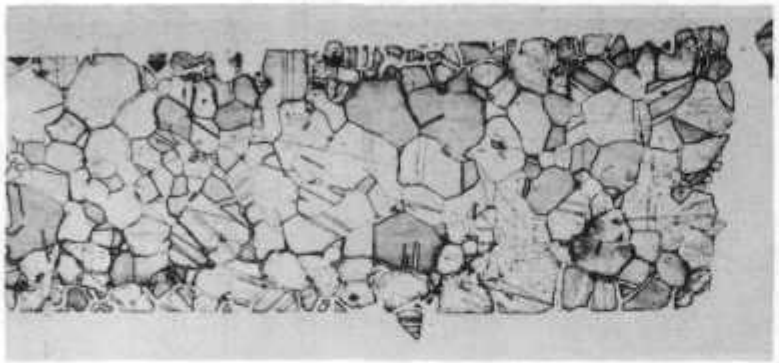

1. E = -1154mV$_H$; T_f = 15.5 hr 150X

Vacuum-annealed

2. E = -1154mV$_H$; T_f = 113 hr 150X

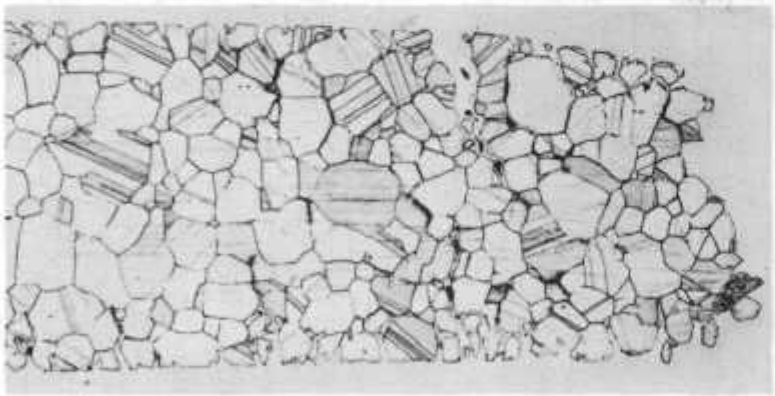

3. E = -1054mV$_H$; T_f = 28.5 hr 150X

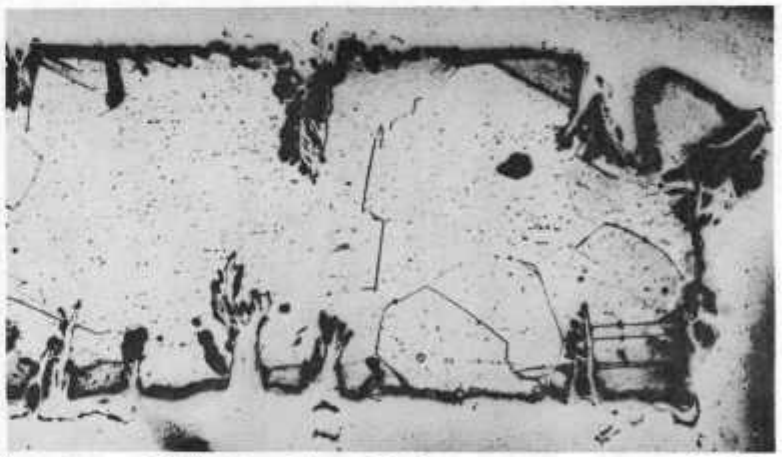

4. E = -1054mV$_H$; T_f = 50 hr 150X

Figure 7 - Effect of Applied Potential on Crack Morphologies of Sensitized and Vacuum Annealed 304 Stainless Steel (Load = 100% of Y.S.)

Sensitized

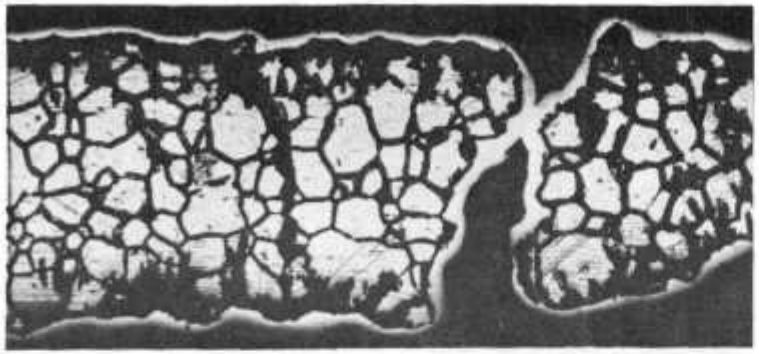

5. 60% NaOH; E = -854mV$_H$; T_f = 15 hr 150X

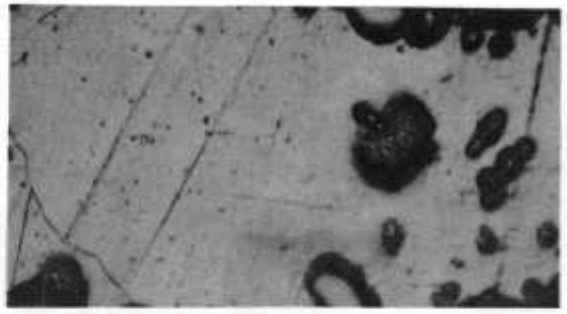

6. 60% NaOH; E = -854mV$_H$; T_f = 42 hr 400X

7. 70% NaOH; E = -854mV$_H$; T_f = 20.25 hr 150X

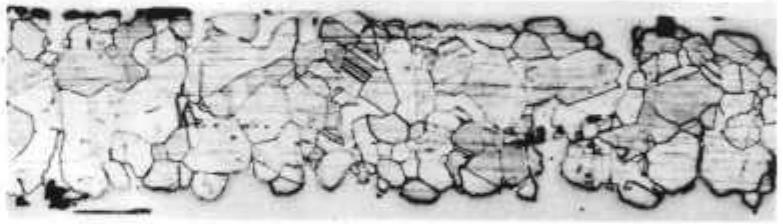

8. 70% NaOH; E = -754mV$_H$; T_f = 34.75 hr 150X

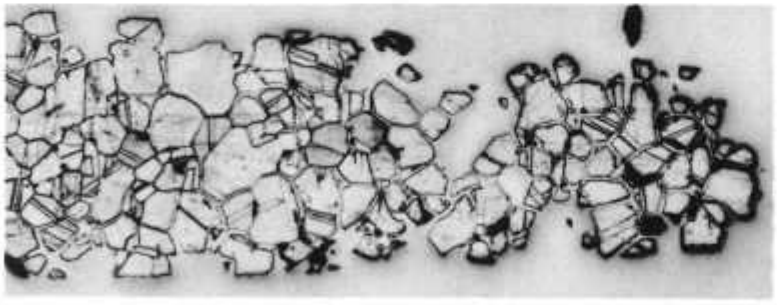

9. 70% NaOH; E = -654mV$_H$; T_f = 25 hr 150X

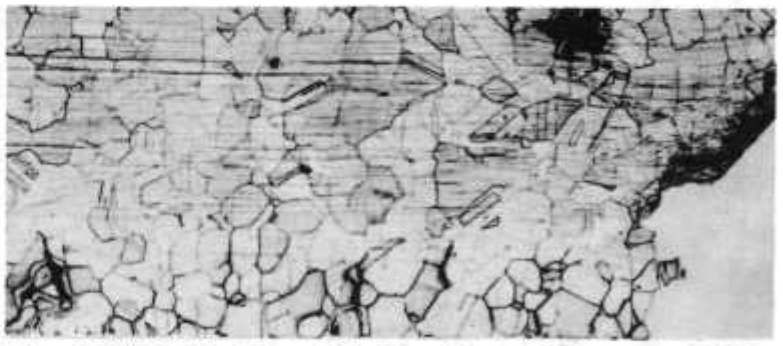

10. 70% NaOH; E = -554mV$_H$; T_f = 23 hr 150X

Figure 7 - Continued

Table II - Effect of Potential on Crack Morphologies

Photo No.	Potential mV(SHE)	Crack Morphology	
		Sensitized	Vacuum Annealed
1&2	-1154	Intergranular--with some brittle cracks (1)	Predominantly transgranular brittle cracks (2)
3&4	-1054	Intergranular--with some brittle cracks (3)	Predominantly transgranular brittle cracks (4)
5&6*	- 854	Mixed type of failure--crack repassivation (5)	Failure by active dissolution
7	- 854	Intergranular--no crack repassivation	
8	- 754	Same as above	
9	- 654	Same as above	
10	- 554	Intergranular	

*60% boiling sodium hydroxide solution

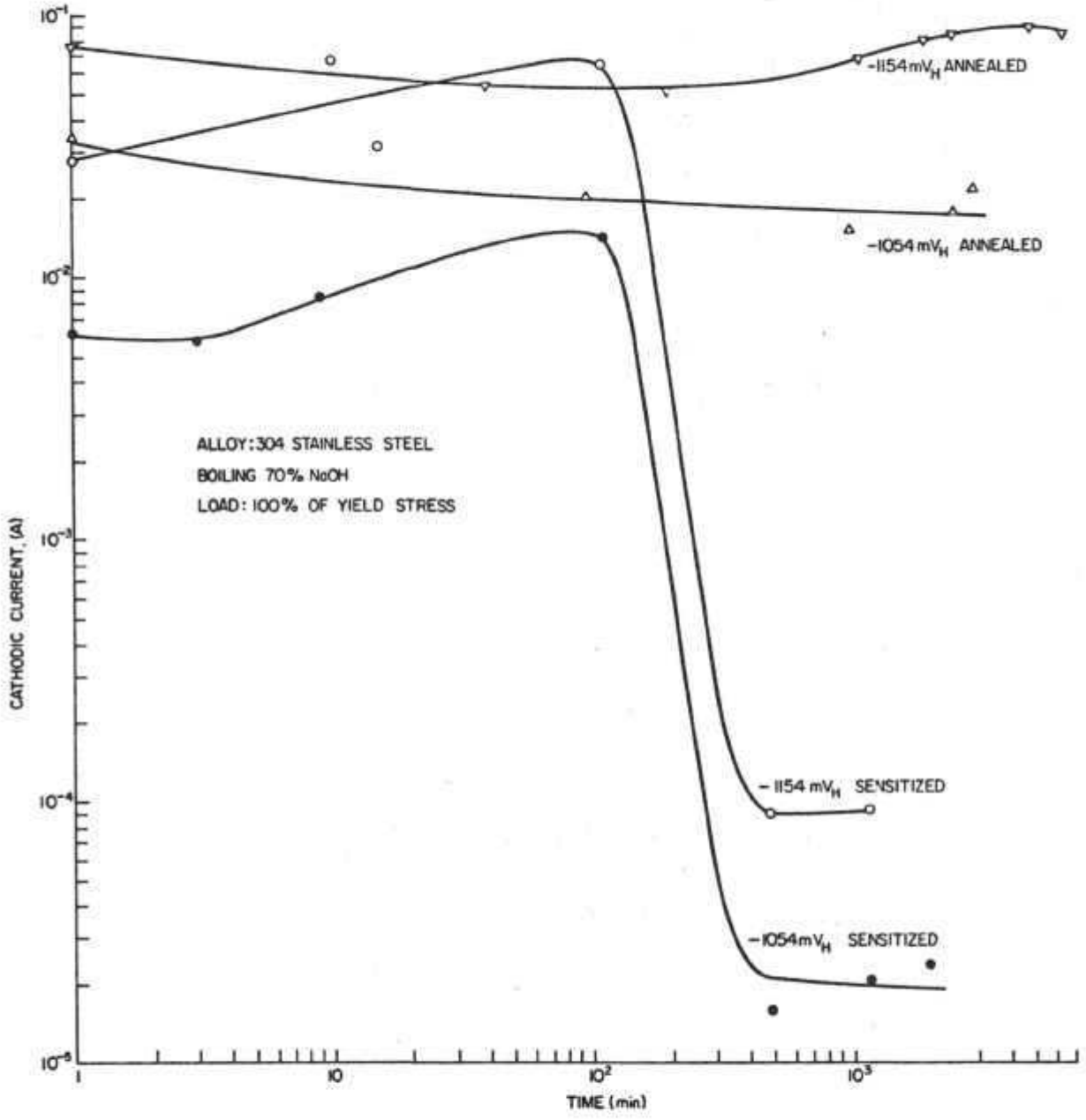

Fig. 8 - Effect of Sensitization on Current-Time Behavior in Cathodic Region

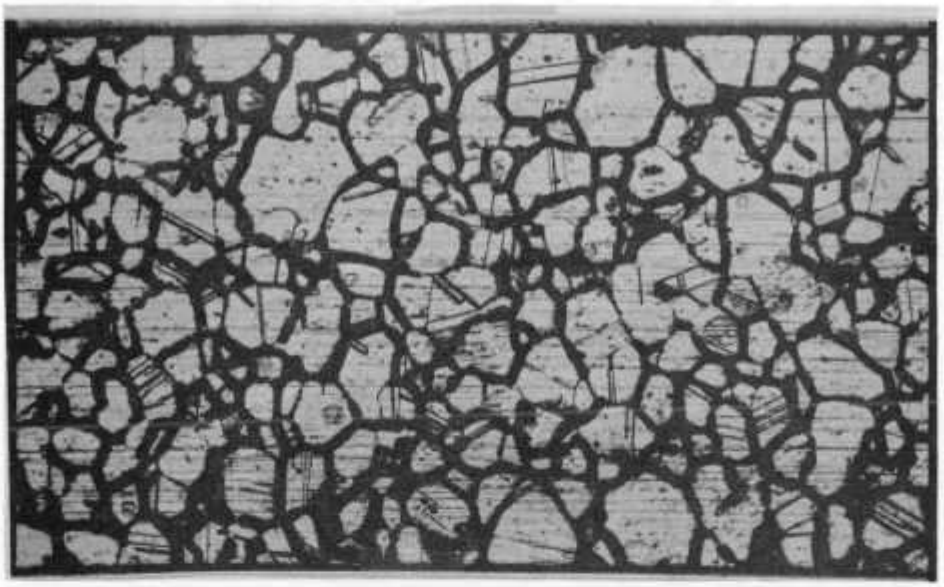

Sensitized at 1100°F for 10 hr and air-cooled 150X

Vacuum annealed - 2200°F for 2 hr and air-cooled 150X

Figure 9 - Effect of Heat Treatment on Structure of 304 Stainless Steel

following equilibrium,

$$2Cr_7C_3 + 21H_2O = 7Cr_2O_3 + 6C(s) + 42H^+ + 42e \qquad (1)$$

and E = -0.489 - 0.0591 pH. In 30% Na)H (pH = 14.8) the equilibirum potential is -1.605 mV at 115°C. The lack of correlation between observed and calculated values indicate that the alternative equilibria could be that governing the formation of CrO_3^{3-} species as given below,

$$Cr_7C_3 + 30H_2O = 7CrO_3^{3-} + 3CO_3^{2-} + 60H^+ + 33e \qquad (2)$$

$$\text{and } E = 0.464 - 0.1182pH + 0.0197 \log[CrO_3^{3-}] \; . \qquad (2)$$

But the above two equilibria give rise to far negative equilibrium potentials, approximately 2-3 V.

Another alternative could be stress assisted intergranular mechanical disintegration of carbide. This assumption is based on the observations of grain boundaries becoming clean upon prolonged exposure to sodium hydroxide (see photomicrographs in Fig. 2). This may possibly account for the potential independence of failure times. The net electrochemical currents observed could be caused by the remaining Fe, Ni and Cr components in the lattice.

Task 3 - General Effect of Alloy and Environmental Composition on Stress Corrosion Cracking in Sodium Base Environments Containing NaOH

A. Aims

The purpose of this task is to perform a parallel program to that in Task 2 except for the environment being a sodium base.

B. Results

None this Quarter.

Task 4 - Dissolution and Passivation Behavior (K. G. Sheth)

A. Aims

This task is aimed at obtaining information on the kinetics of oxidation and reduction processes in electrochemically accessible (i.e., ionically conducting) environments. This includes aqueous and fused salt environments as opposed to liquid metals. This work will

define those regions where activated dissolution and passivation occurs as a function of alloy, temperature, and environmental composition. The definition of these regions will provide a guide to where stress corrosion might occur and also will provide direct information on corrosion rates.

B. Results

1. Introduction

The present work is to investigate the effects of temperature, pH, and alloy concentration on the polarization behavior of Fe-Ni and (Fe + 20Cr) - Ni alloys. Compositions of various alloys used for this investigation are given in a previous report. These alloys were selected with a view in mind to study the effect of nickel in Fe-Ni.

The corrodent or the electrolyte used for these investigations was 1, 5, and 10N NaOH. Temperatures studied were in the range 25-90°C.

Results of anodic polarization studies were reported in COO-2018-18(Q-5). In this report results of cathodic polarization studies are presented.

2. Experimental

The experimental set up and procedure was similar to that described elsewhere.[5,6] Cathodic polarization was performed at 600 mV/hr, starting at the corrosion potential of the sample and ending in the hydrogen evolution region.

3. Results

Cathodic polarization curves of alloys #2, 3, 4, 12, 51, 55, 58, and 62 at 70°C in caustic solutions of strength 1, 5, and 10N are shown in Figs. 10 to 15. In these figures polarization curves of several alloys are plotted together to show the effect of composition. The effect of temperature on polarization behavior of individual alloys in 10N NaOH are shown in Figs. 16 to 23. Tafel slopes for hydrogen evolution reaction (HER) obtained from the above figures are listed in Tables III and IV as a function of caustic concentration and temperature, respectively.

Cathodic polarization curves in Figs. 10 to 23 all show identical behaviors. There are two distinct regions, a) oxide reduction region, where the surface oxides on the samples are reduced; and b) hydrogen evolution region, where, after the oxides have been reduced, hydrogen evolution occurs. In almost all cases, oxide reduction was complete at potentials of -1.1 V(SCE). There appears to be no significant trend in polarization curves because of Ni addition.

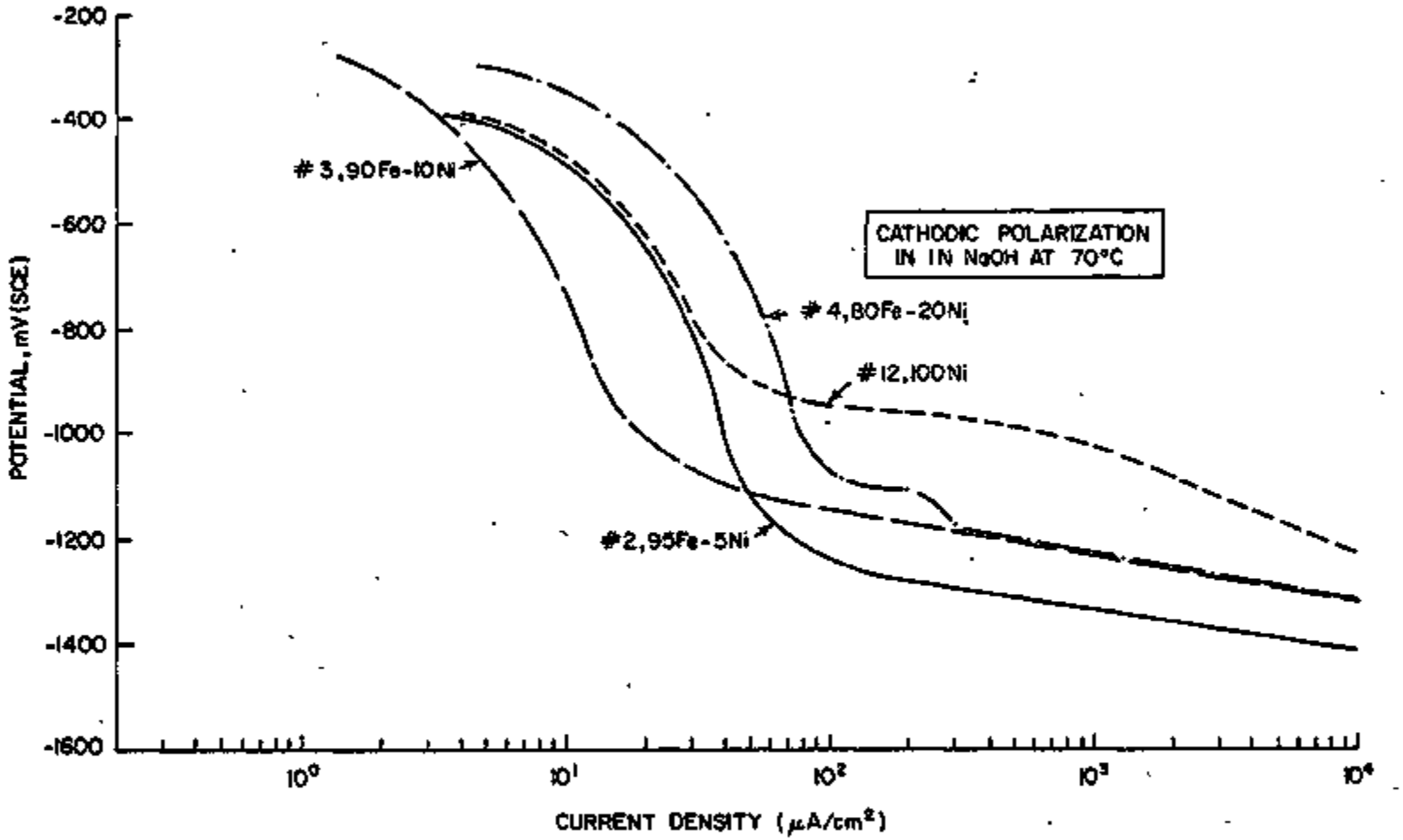

Fig. 10 - Cathodic Polarization Behavior in 1N NaOH at 70°C

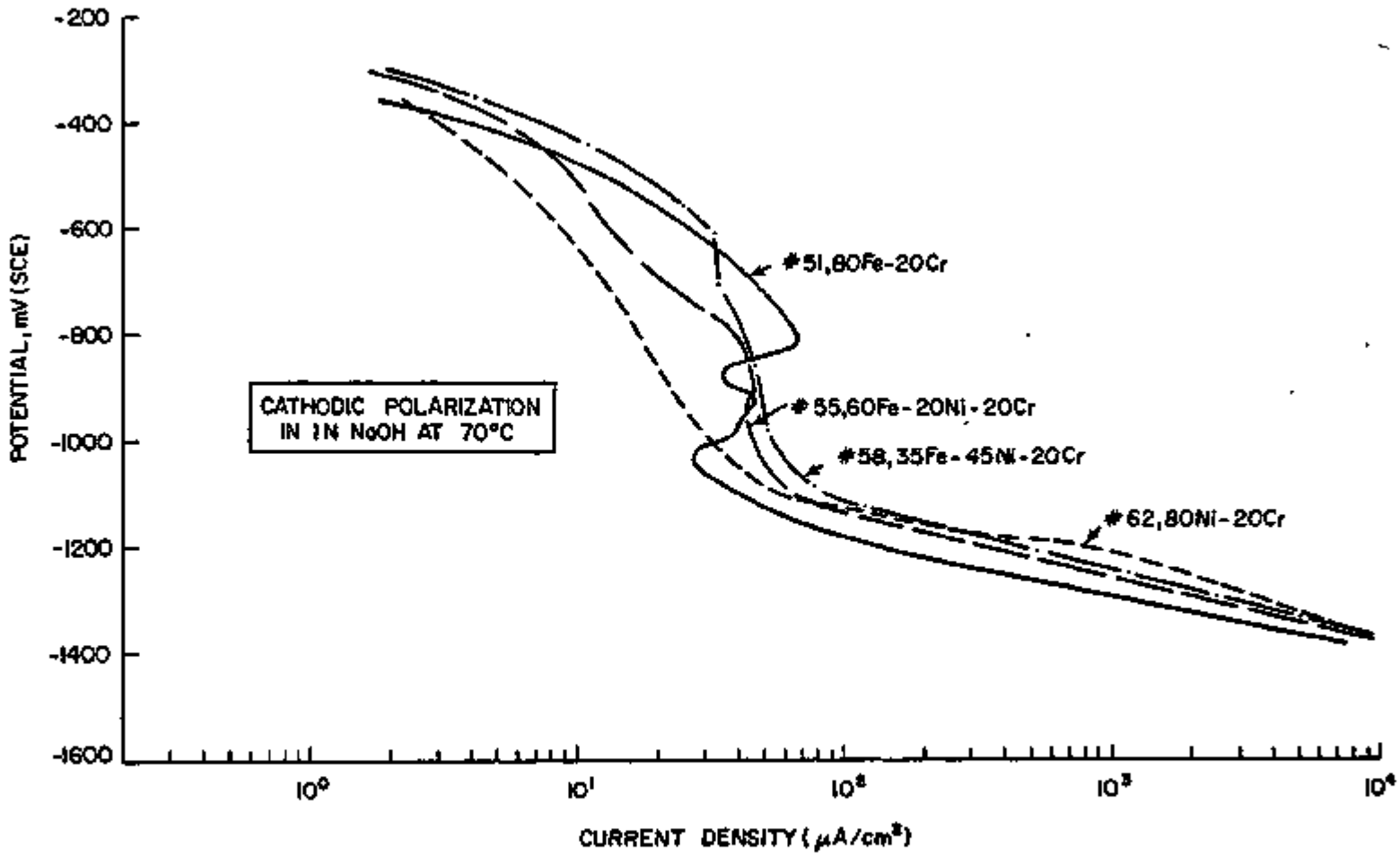

Fig. 11 - Cathodic Polarization Behavior in 1N NaOH at 70°C

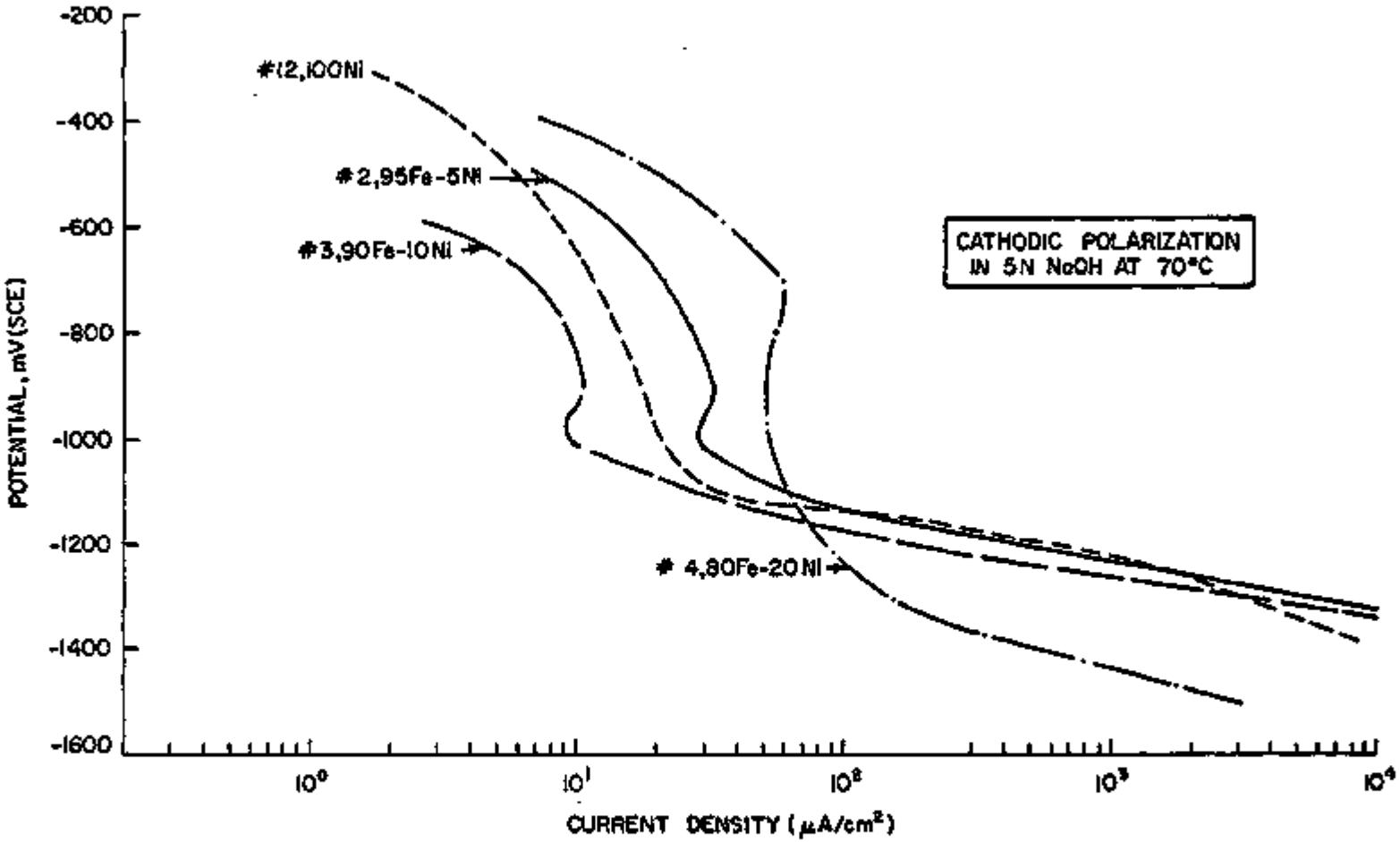

Fig. 12 - Cathodic Polarization Behavior in 5N NaOH at 70°C

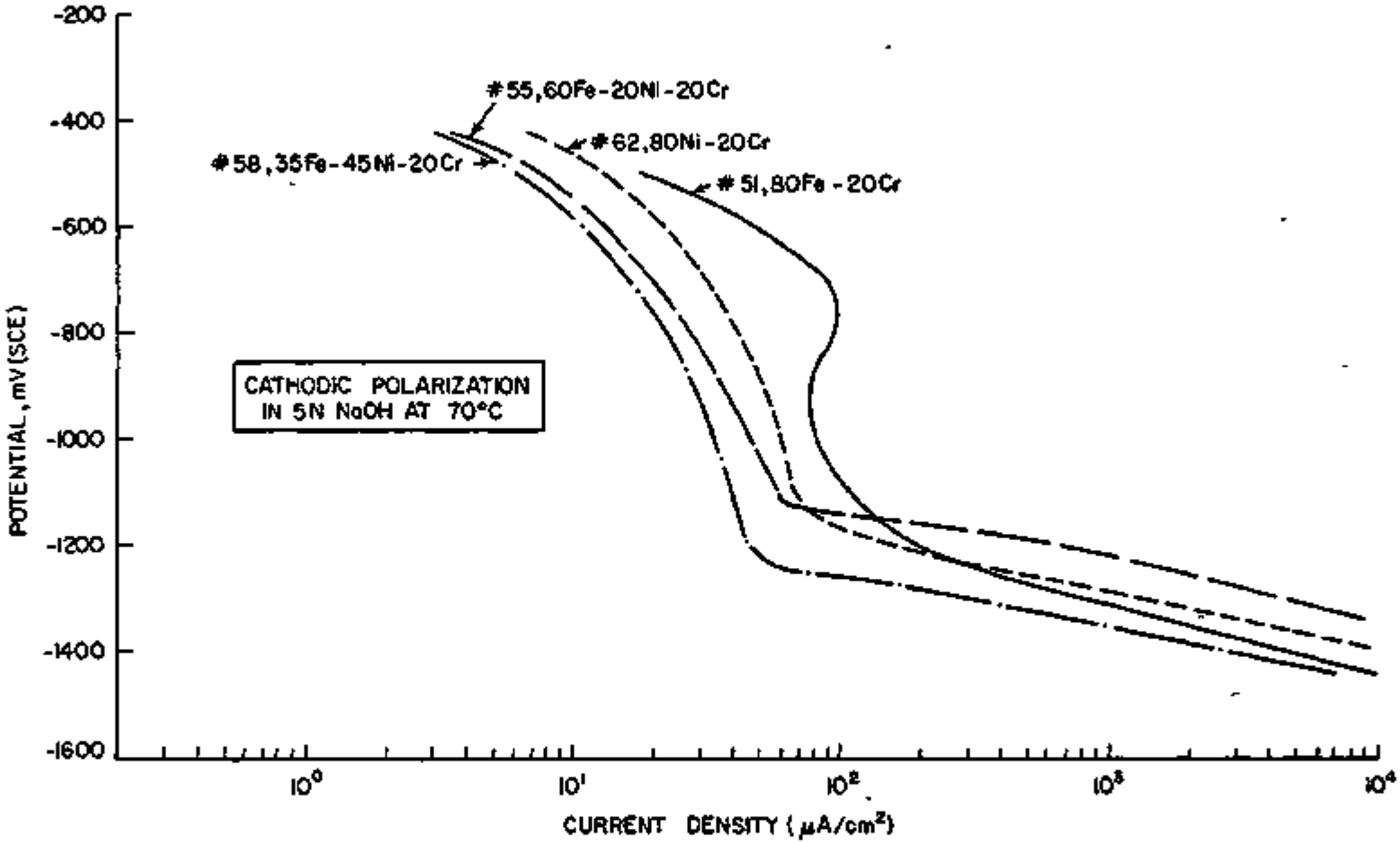

Fig. 13 - Cathodic Polarization Behavior in 5N NaOH at 70°C

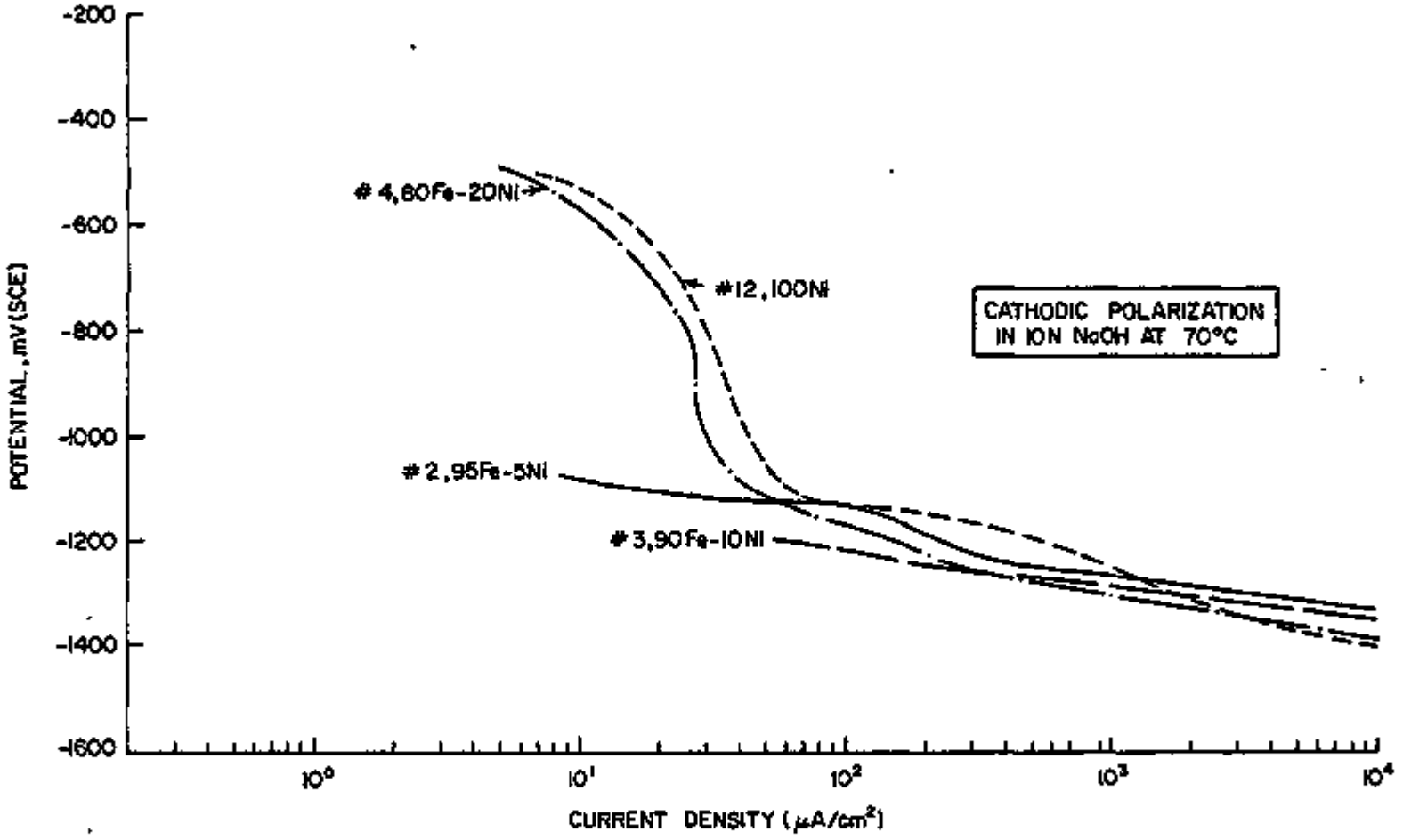

Fig. 14 - Cathodic Polarization Behavior in 10N NaOH at 70°C

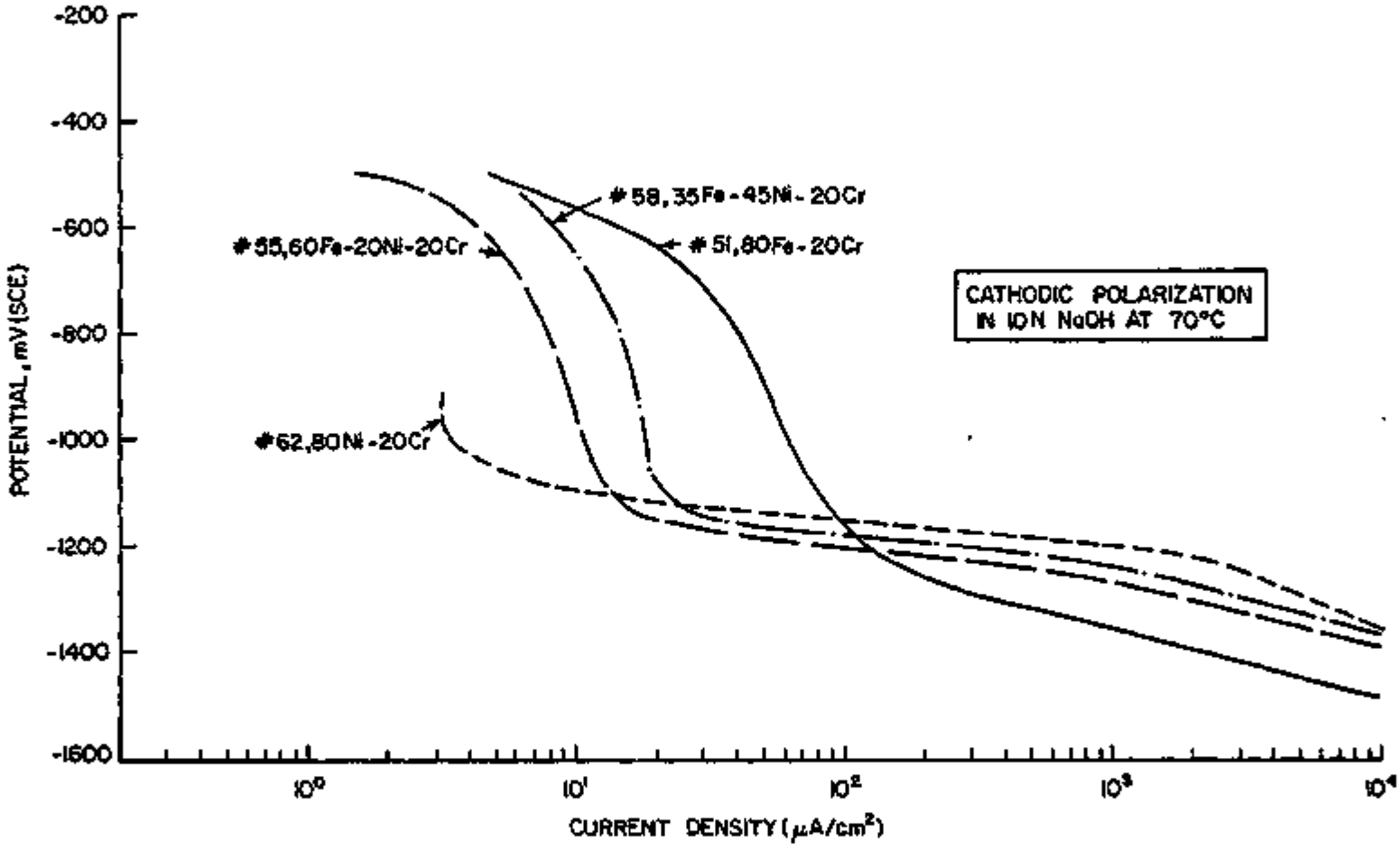

Fig. 15 - Cathodic Polarization Behavior in 10N NaOH at 70°C

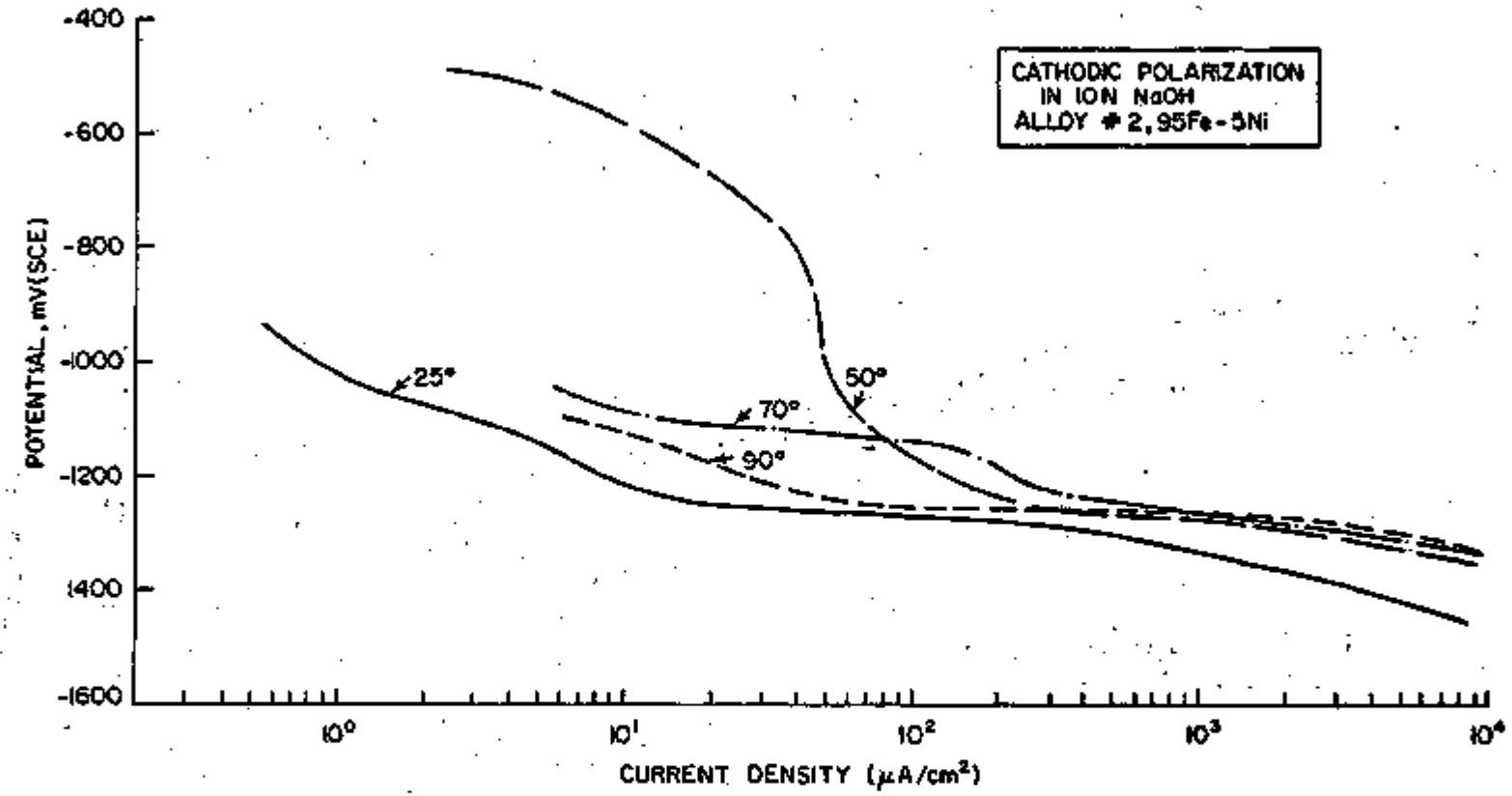

Fig. 16 - Effect of Temperature on Cathodic Polarization Behavior of Alloy # 2 in 10N NaOH

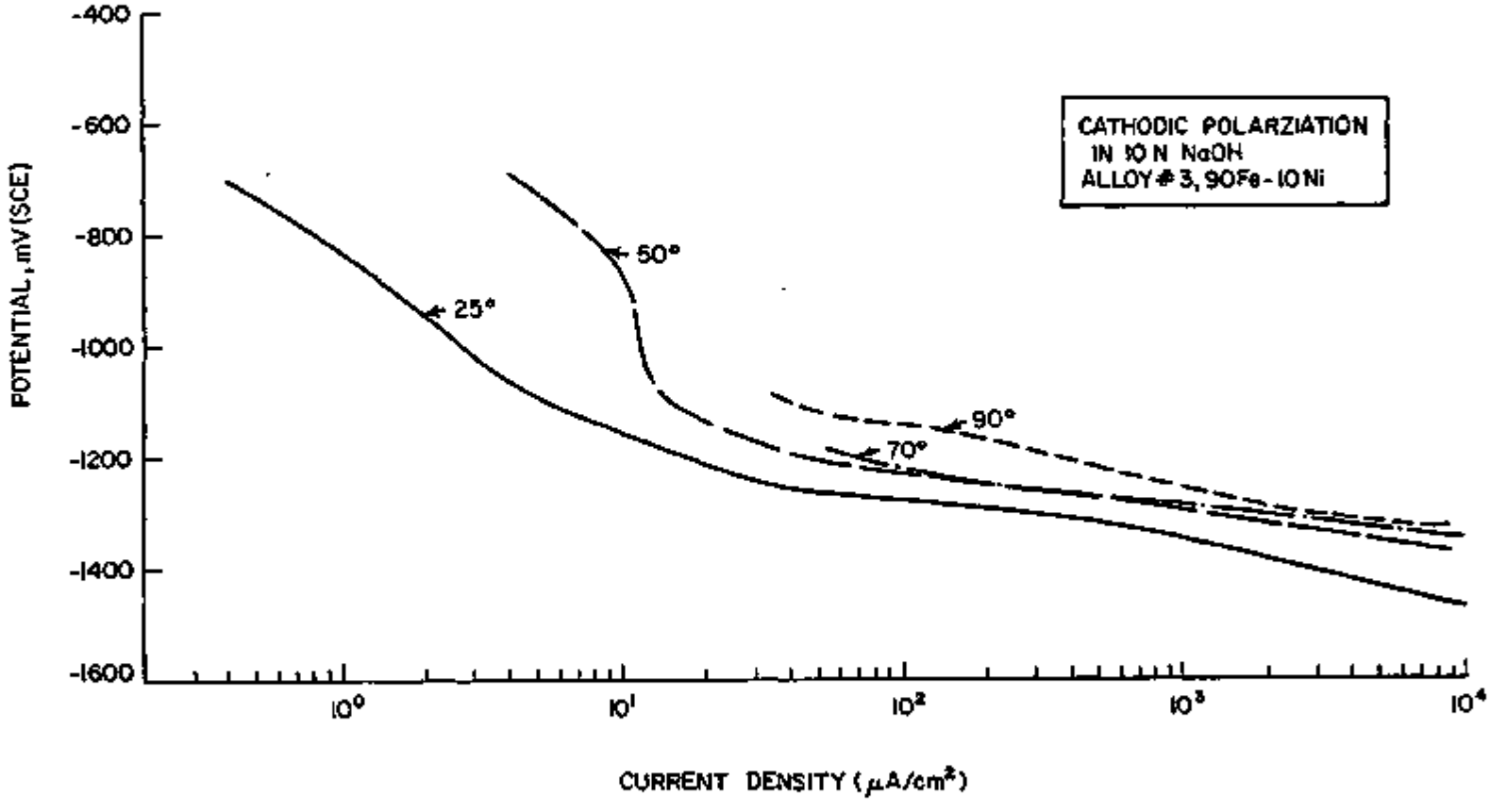

Fig. 17 - Effect of Temperature on Cathodic Polarization of Behavior of Alloy # 3 in 10N NaOH

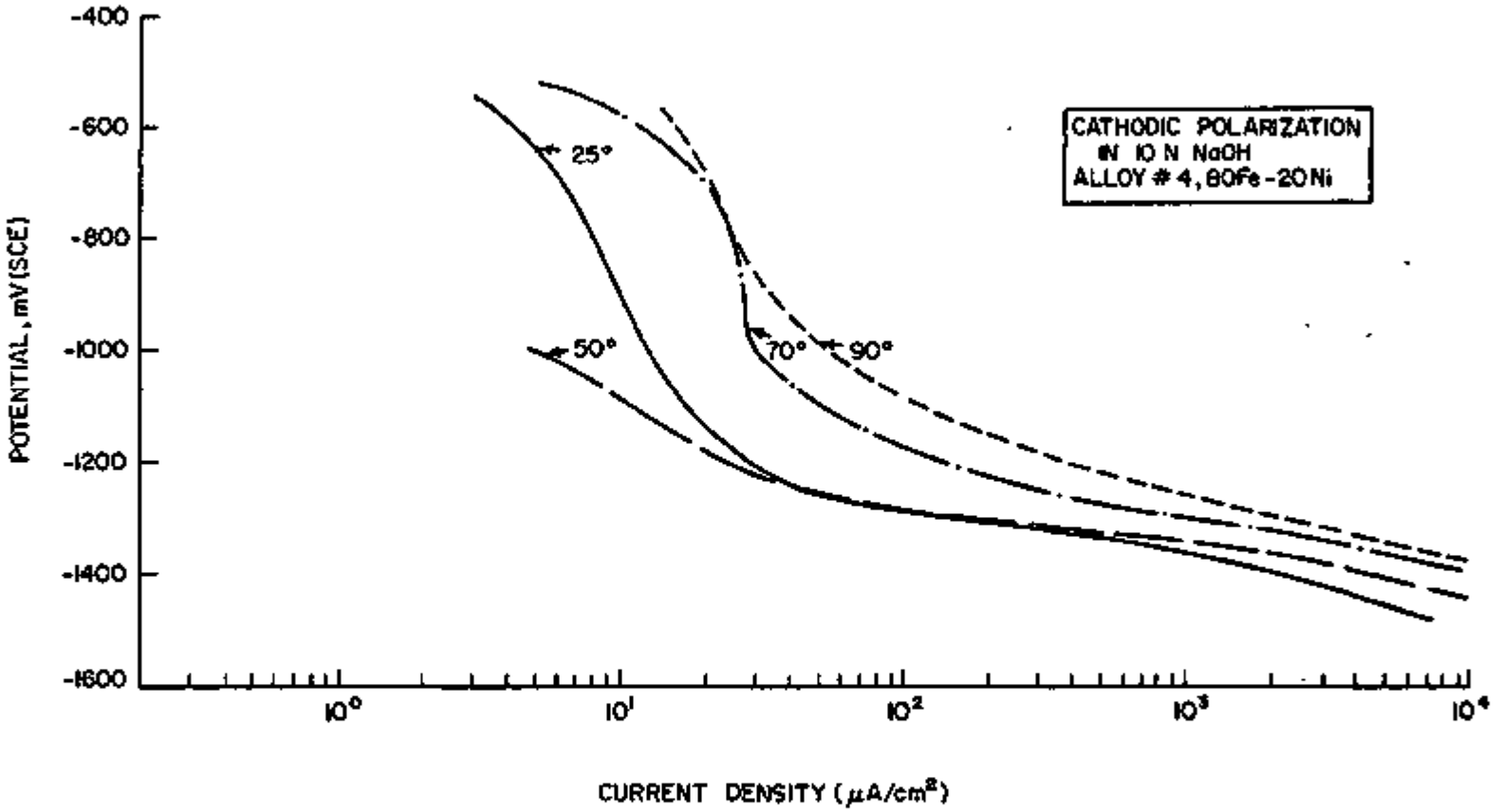

Fig. 18 - Effect of Temperature on Cathodic Polarization Behavior of Alloy #4 in 10N NaOH

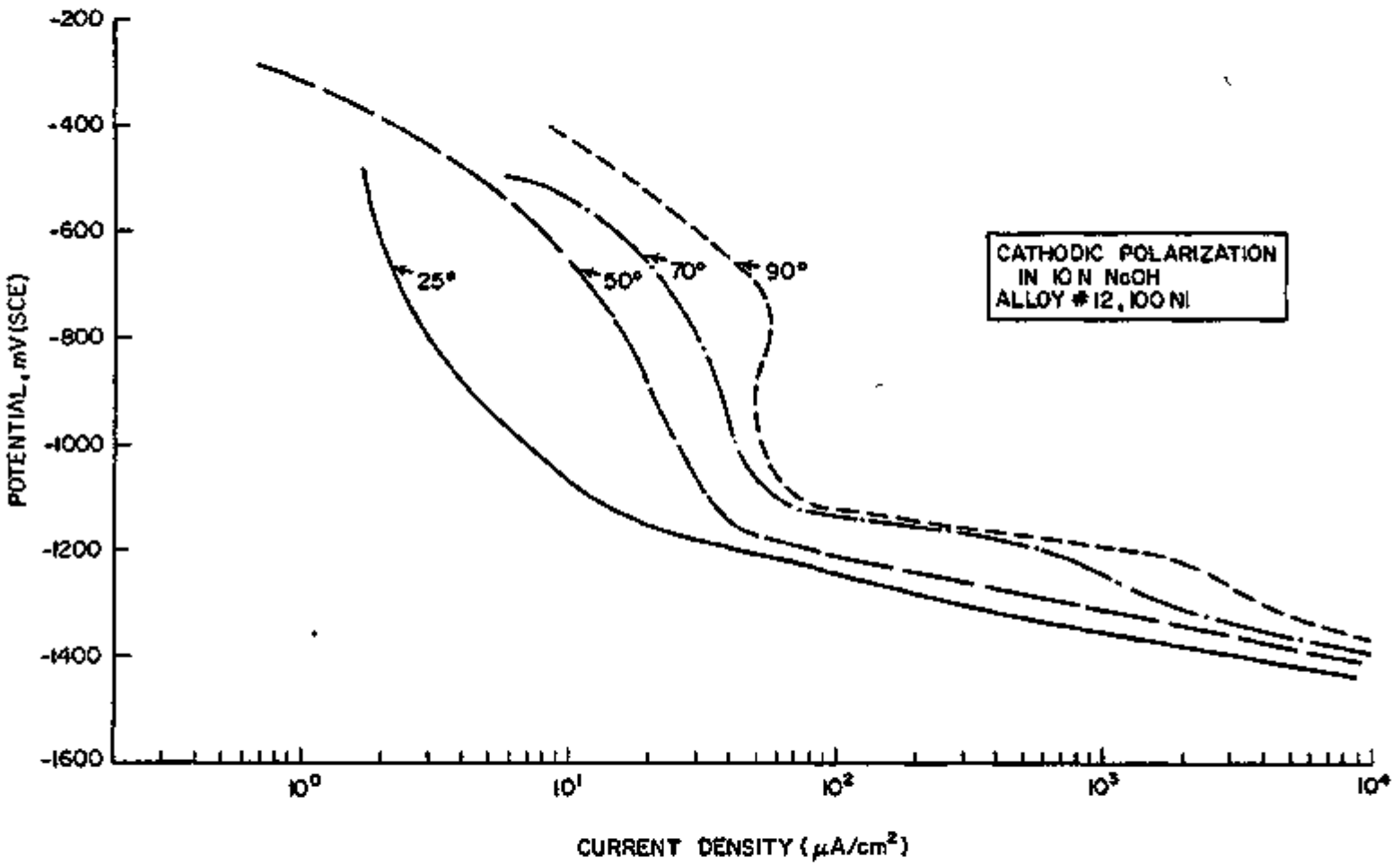

Fig. 19 - Effect of Temperature on Cathodic Polarization Behavior of Alloy #12 in 10N NaOH

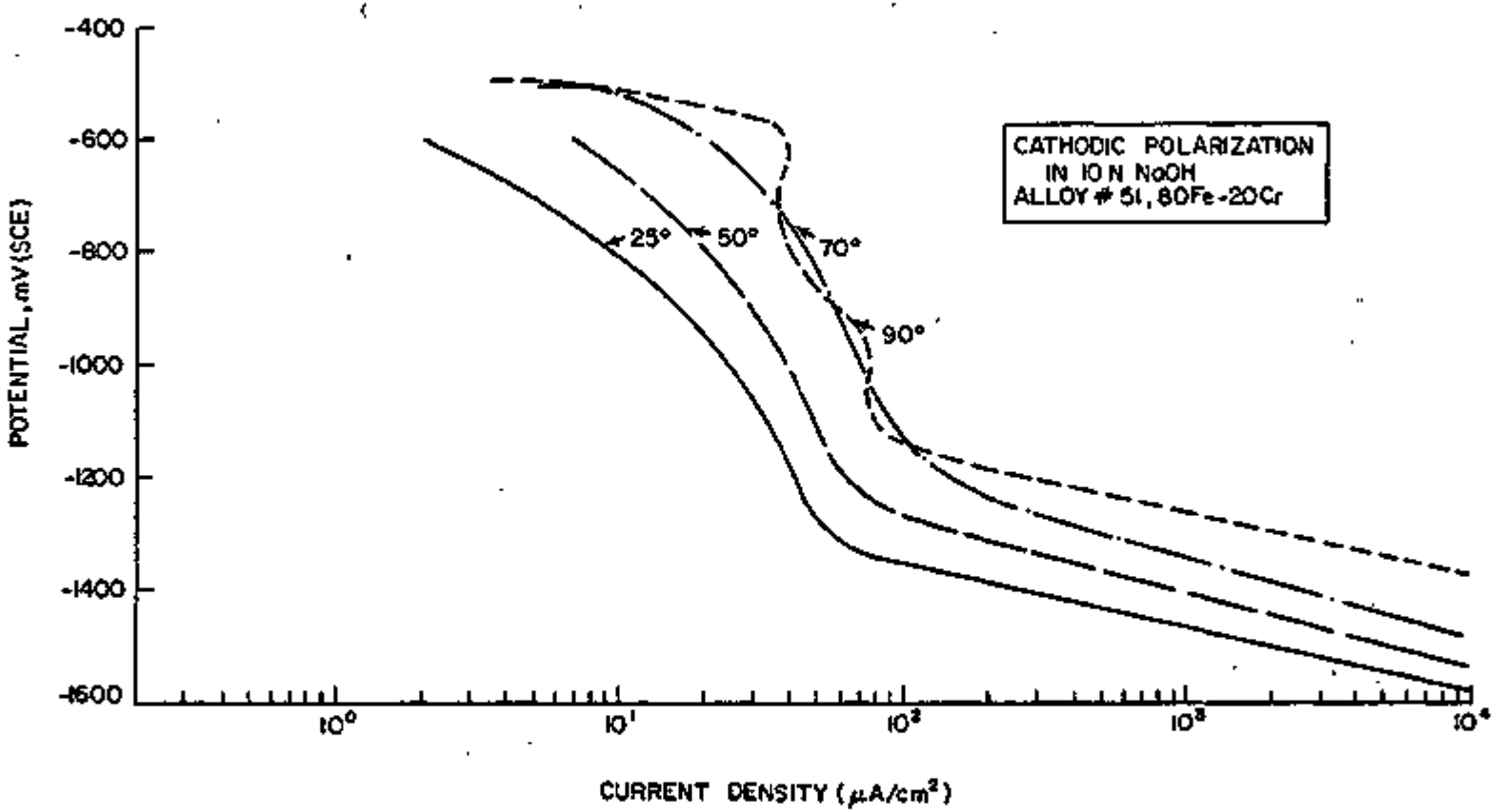

Fig. 20 - Effect of Temperature on Cathodic Polarization Behavior of Alloy #51 in 10N NaOH

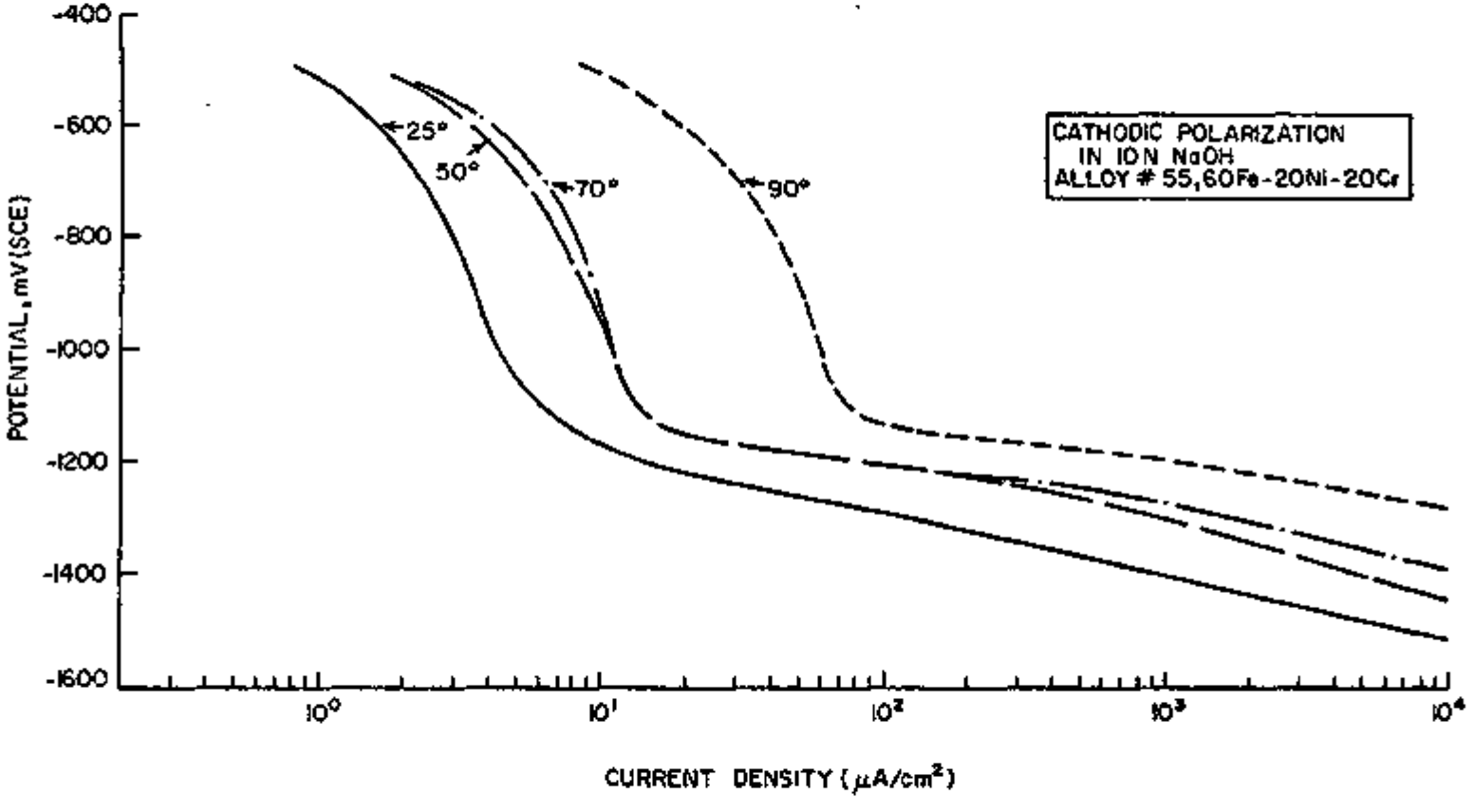

Fig. 21 - Effect of Temperature on Cathodic Polarization Behavior of Alloy #55 in 10N NaOH

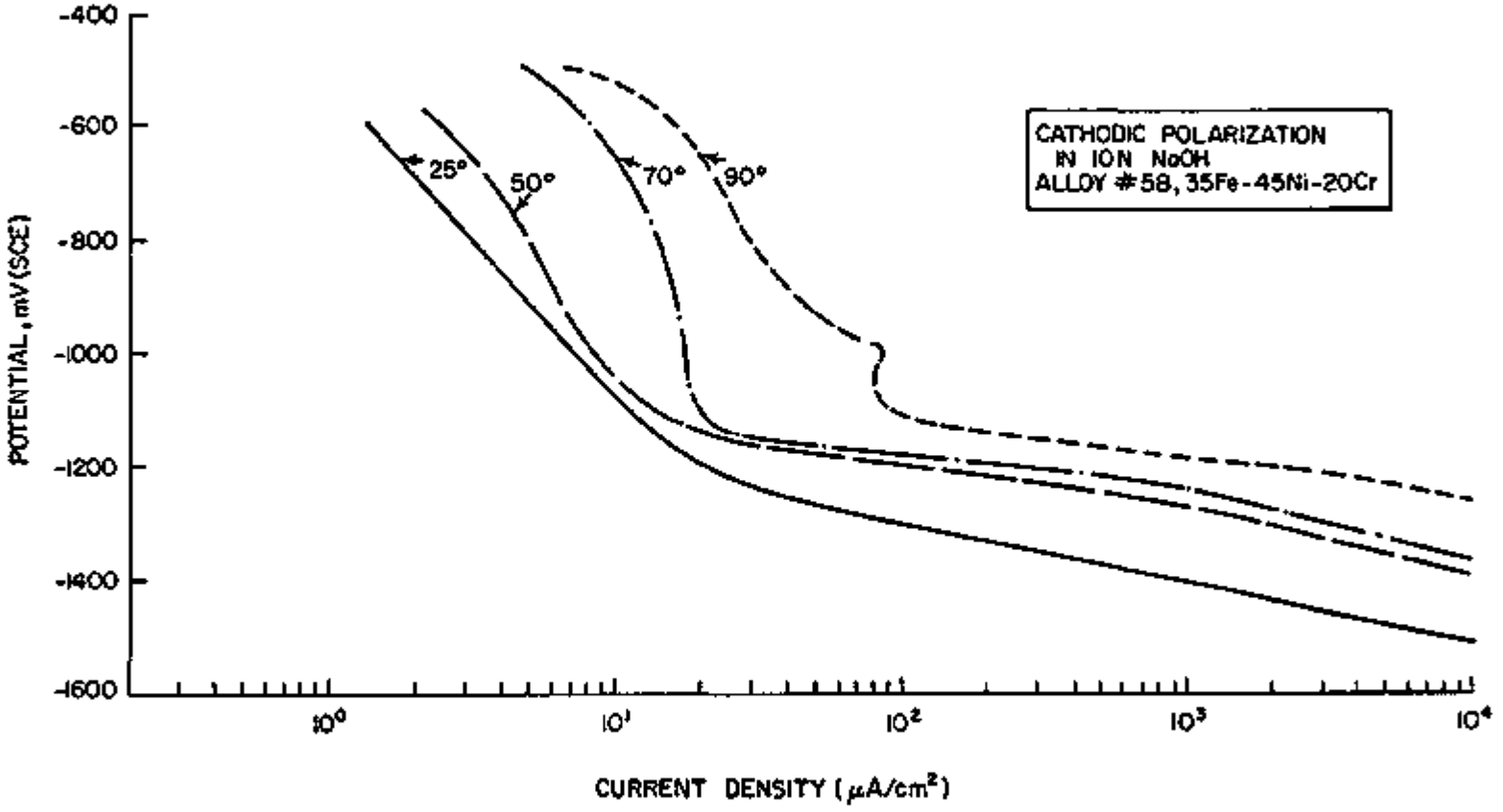

Fig. 22 - Effect of Temperature on Cathodic Polarization Behavior of Alloy #58 in 10N NaOH

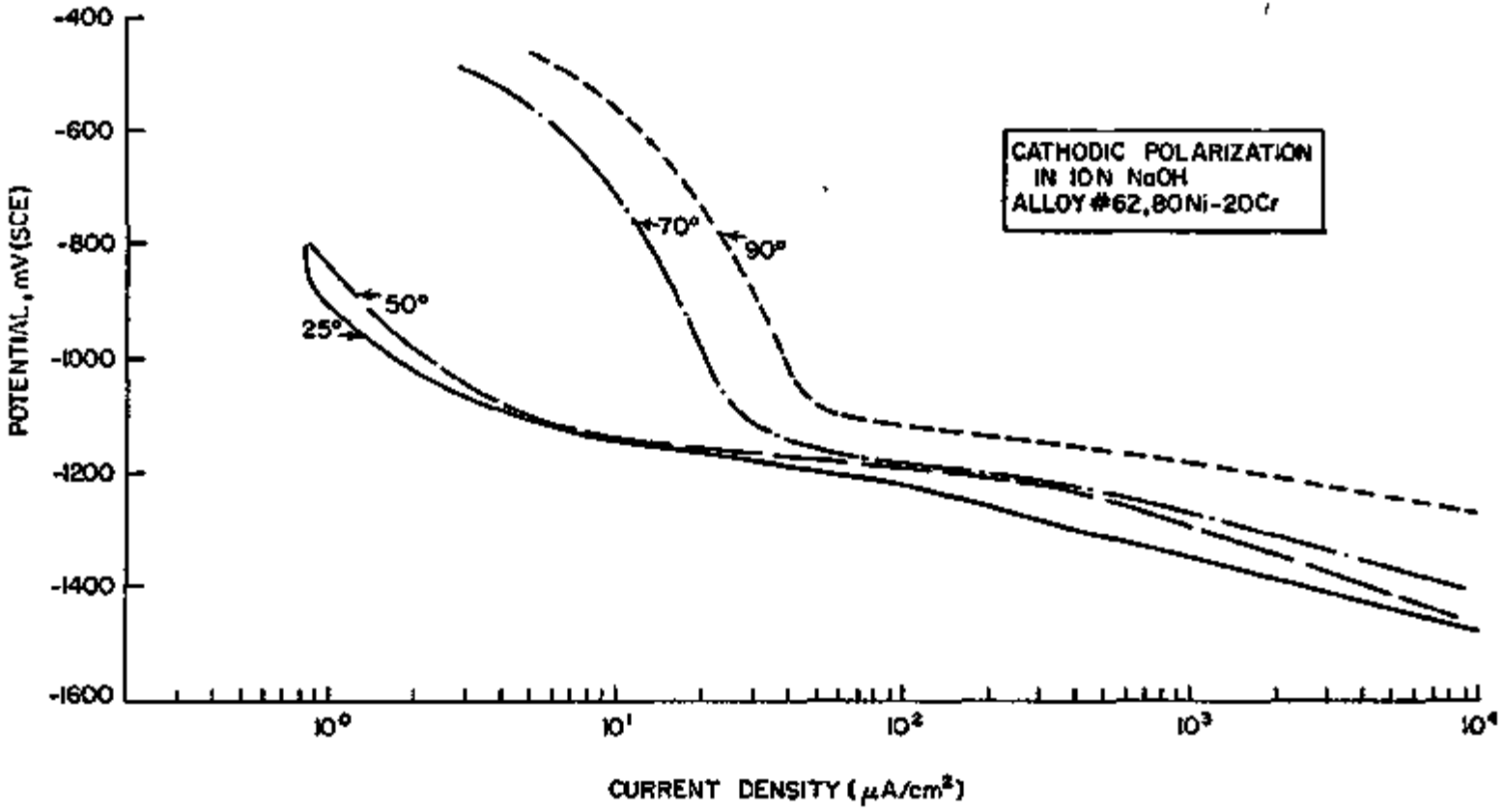

Fig. 23 - Effect of Temperature on Cathodic Polarization Behavior of Alloy #62 in 10N NaOH

Table III - Tafel Slopes for HER in Various Caustic Solutions at 70°C

Alloy No.	Slope, b (mV)		
	Caustic Concentration		
	1N	5N	10N
2	80	85	75
3	90	75	62
4	90	125	90
12	100	~ 100	~ 90
51	110	135	125
55	115	90	75
58	125	110	125
62	100	100	100

Table IV - Tafel Slopes for HER at Various Temperatures in 10N NaOH

Alloy No.	Slope, b (mV)			
	Temperature (°C)			
	25	50	70	90
2	100	~ 75	~75	~ 75
3	125	80	62	110
4	130	100	90	125
12	100	~ 100	~ 100	~ 100
51	110	120	125	115
55	112	137	110	75
58	125	125	125	75
62	130	130	100	80

Caustic concentration had little effect on hydrogen evolution reaction. O'Brien and Seto[7] polarized commercial 304 stainless steel in caustic solutions of strength 0.1-10M, and reported that HER potential shifts to slightly noble side with increasing concentrations. In their case, solutions were saturated with helium which might have caused this change.

Increase in temperature was found to shift HER potentials to more noble side (Figs. 16 to 23). The potential shift was approximately 150 mV when temperature changed from 25 to 90°C; this trend is in agreement with that reported in literature. Batarakov et al.[8] have studied the cathodic polarization of Fe in 5N KOH as a function of temperature in the range -20 to +20°C, and have reported that the increase in temperature shifted HER potential to more noble values.

Tafel slopes for HER of the alloys were in the range of 75-135 mV. With a few exceptions, addition of Ni to Fe-Ni and Fe-Cr-Ni increased their Tafel slopes; whereas, in general, increase in caustic concentration and temperature decreased the Tafel slopes. Although HER has been studied on pure metals, there are few comparable works on Fe-Ni-Cr alloys. Tafel slopes obtained by O'Brien and Seto[7] fall in the range of 105-134 mV and, thus, are in agreement with the present work. It is interesting to mention in their findings that addition of NaF, NaCl, NaI, $BaCl_2$, and $LaCl_3$ did not significantly affect the rate of hydrogen evolution. O'Brien and Seto reported that the anions F^-, Cl^-, and I^- were probably repelled from the highly negatively charged metal surface.

The results of cathodic polarization studies will be useful in applying cathodic protection to metals, and also in avoiding metal failures because of hydrogen embrittlement.

Task 5 - Effect of Environment on Mechanistic Behavior

(F. O. Du)

A. Aims

The aim of this work is to find the effects of environmental variables on the course of mechanistic processes associated with caustic SCC. This work emphasizes effects of environmental chemistry, as opposed to Task 7 which emphasizes effects of metallurgical variables. This work also helps to interpret work in Task 6.

B. Results

1. Introduction

The outline of the experiments and the design of the apparatus to be used for this task are presented.

Fused sodium hydroxide is possibly a good coolant for nuclear power reactors since a) it has good heat transfer and fluid flow characteristics; b) it has good moderating ability because of its stability at high temperatures with respect to both thermal dissociation and radiation damage;[8] c) its vapor pressure is low at high temperatures; d) it has comparatively small cross section for capture of thermal neutrons; and finally, e) it is readily available and economically cheap as compared to other coolants.

To date little information is available on the behavior of structural materials in the aggressively corrosive environment of fused NaOH. The early work[10-15] done at Battelle Memorial Institute, Oak Ridge National Laboratory, and Lewis Flight Propulsion Laboratory was directed primarily toward finding suitable containers for fused NaOH. Most of these data are still classified.[16-25]

The first goal of this work is to evaluate the behavior of structural materials under stress in fused NaOH system. Hopefully, data obtained will designate the best type of alloy for this system. The second goal is to understand the mechanism that takes place prior to the onset of crack propagation. Analysis of data can possibly answer some of the questions speculatively posed. The following are a few examples: Does the material start to crack due to embrittlement caused by the environment? Is it because the alloy undergoes a rapid thinning and suddenly cannot support the high stresses from the constant load? If so, what is the mechanism of rapid thinning? Could general corrosion be due to large solubility at elevated temperatures? Is there a threshold stress below which SCC does not occur? What is the stress level at which onset of crack propagation ensues? A host of other interesting questions could be enumerated. The answers will lie in the evidence provided by data gathered.

2. Experimental

Three types of SCC tests are proposed to be performed on five different alloys: (1) Static bending SCC test, (2) static tensile SCC test, and (3) dynamic SCC test. The alloys chosen for investigation are SS304, SS430, Incoloy 800, Inconel 600, and Croloy (2¼% Cr + 1% Mo). The information sought from these experiments is:

a. Weight changes per unit area and their corresponding dimensional changes.

b. The influence of stress level on rupture time.

c. The influence of bath temperature on rupture time.

d. The specimen having highest resistance to SCC.

e. Metallographic analysis of corrosion products.

f. Length of crack, number of cracks, maximum crack depth as a function of time, stress level and bath temperature.

g. Embrittlement test of specimen by microhardness testing of the inner surfaces. Other techniques, such as etching, may be employed to reveal microstructural changes.

h. Other undesirable changes in mechanical properties of the thin sections.

i. Onset of cracking by plotting total number of cracks vs. stress level and extrapolation of the curve.

j. Onset of cracking by analysis of recorder readings.

k. Potential vs. time diagram of specimens pulled in tension at constant load.

l. Influence of stress levels on the potential of specimens at constant temperature.

(a) Apparatus and specimens--Design of the apparatus is given in Fig. 24. The alloy specimens are in the form of annealed sheets milled to sizes shown in Figs. 25 and 26.

(b) Experimental operating temperatures--The melting point of pure fused NaOH is 320°C. However, Normal Fast Breeder Reactor operates in the temperature range 450 to 800°C. It is, therefore, planned to investigate this full range of temperature.

(c) Blanketing atmosphere--NaOH is very hygroscopic and can readily absorb moisture and CO_2 from the air. It is, therefore, necessary to protect the fused NaOH from exposure to air during the course of the experiment. Any of the following inert gases can be used in this investigation for providing a blanketing atmosphere;

Argon--Used in systems where a heavy gas is desirable. It tends to protect open-lidded vessels.

Helium--Principally used as a cover gas for a nuclear power system, thus if close simulation to reactor conditions are aspired, this gas should be used.

Nitrogen--The cover gas recommended for most applications, mainly because it is the least expensive.

(d) Reference electrode--In 1921, Baum[26] was the first to use an inert alloy electrode in fused NaOH for the measurement of relative potentials. It was observed by Agar and Bouden[27], and later by Lux,[28,29] that an inert electrode could be used to follow the progress of a reaction by measuring the change in potential between a reference

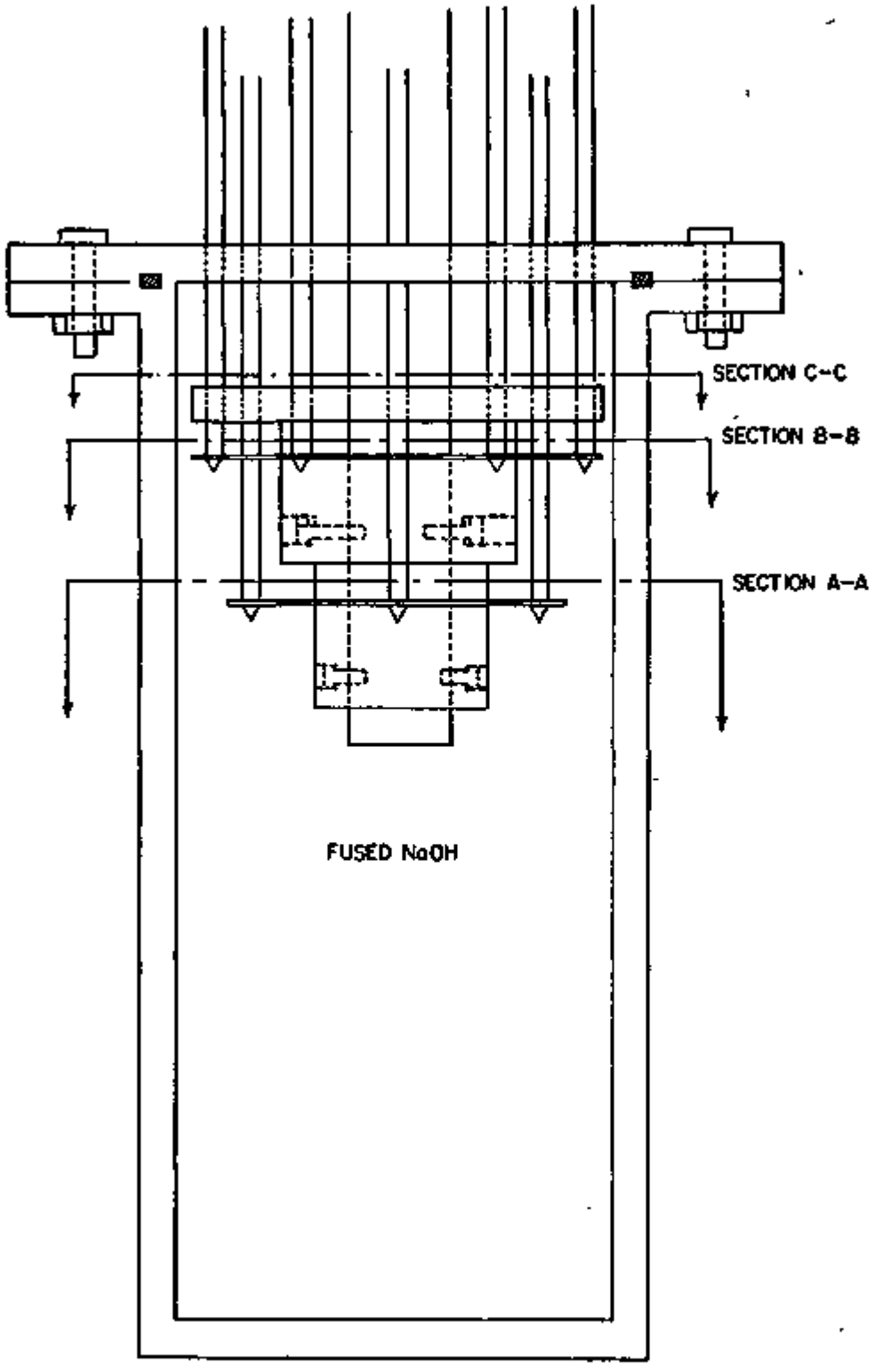

Fig. 24-A - Side View of the Bending Apparatus Fitted into a Crucible Furnace

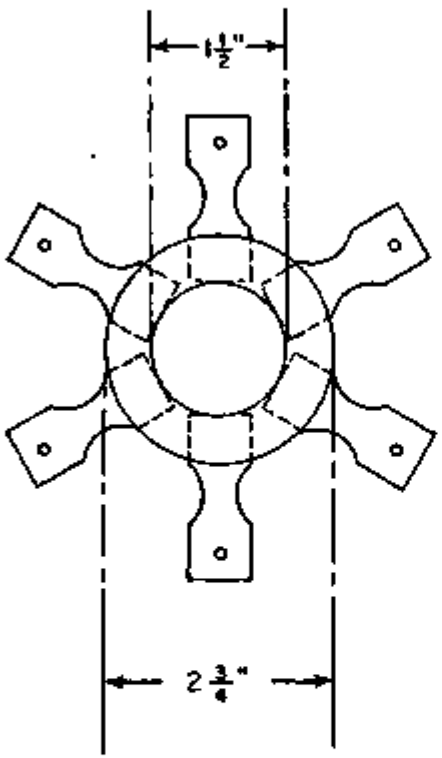

SECTION A—A

Fig. 24-B - Top Sectional View of the Bending Apparatus

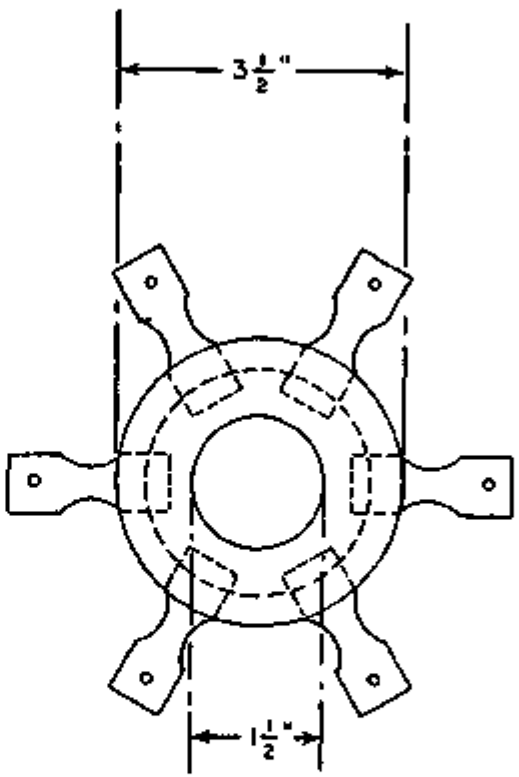

SECTION B-B

Fig. 24-C - Top Sectional View of the Bending Apparatus

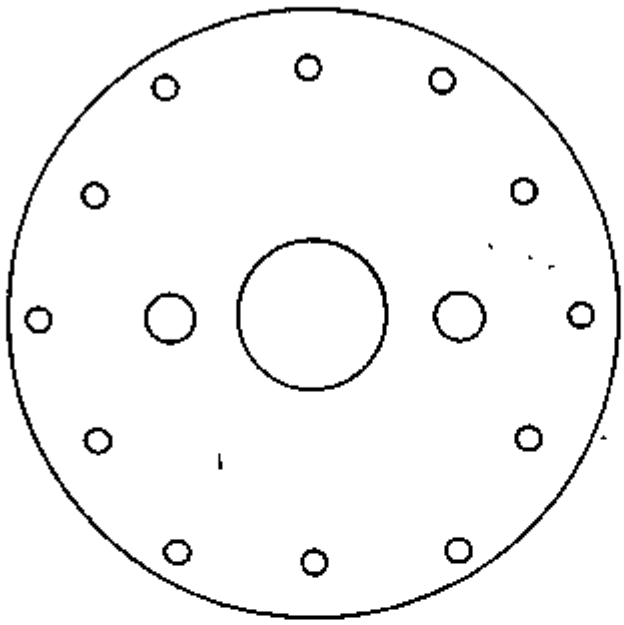

SECTION C—C

Fig. 24-D - Top View of the Guide Plate

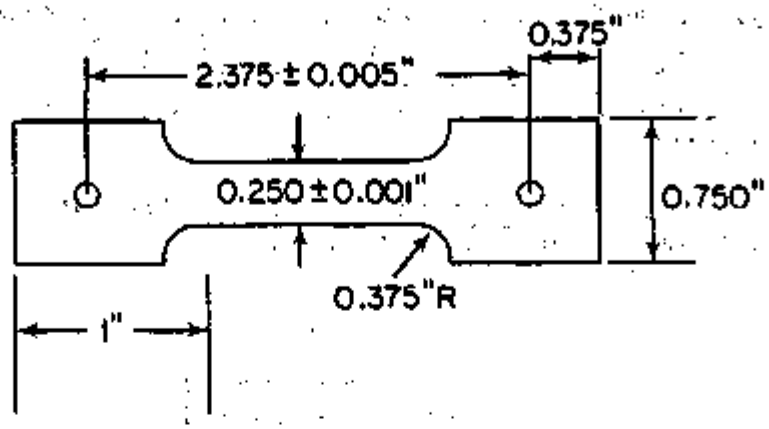

Fig. 25 - Specimen's Shape and Dimensions for the Tensile Test

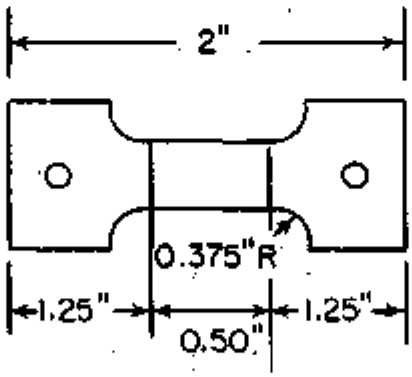

Fig. 26 - Specimen's Shape and Dimensions for the Bending Test

and an indicator electrode. They have shown that the deposition of oxygen from fused sodium hydroxide is accompanied by a considerable overpotential, and this overpotential varies in an orderly manner with the current density. The reference electrode, which was a fine wire of either gold or platinum, acted as a reversible oxygen electrode. The nickel container (pot) itself served as the cathode. The overpotential is given directly by the potential difference between the anode and the reversible reference electrode. Recently, Ivan Dirmoik[30] and Stern and Carlton[31] used the same technique. This technique could also be employed in the present investigations.

(e) Strain gauges and recorders: The following block diagram shows the various equipments required:

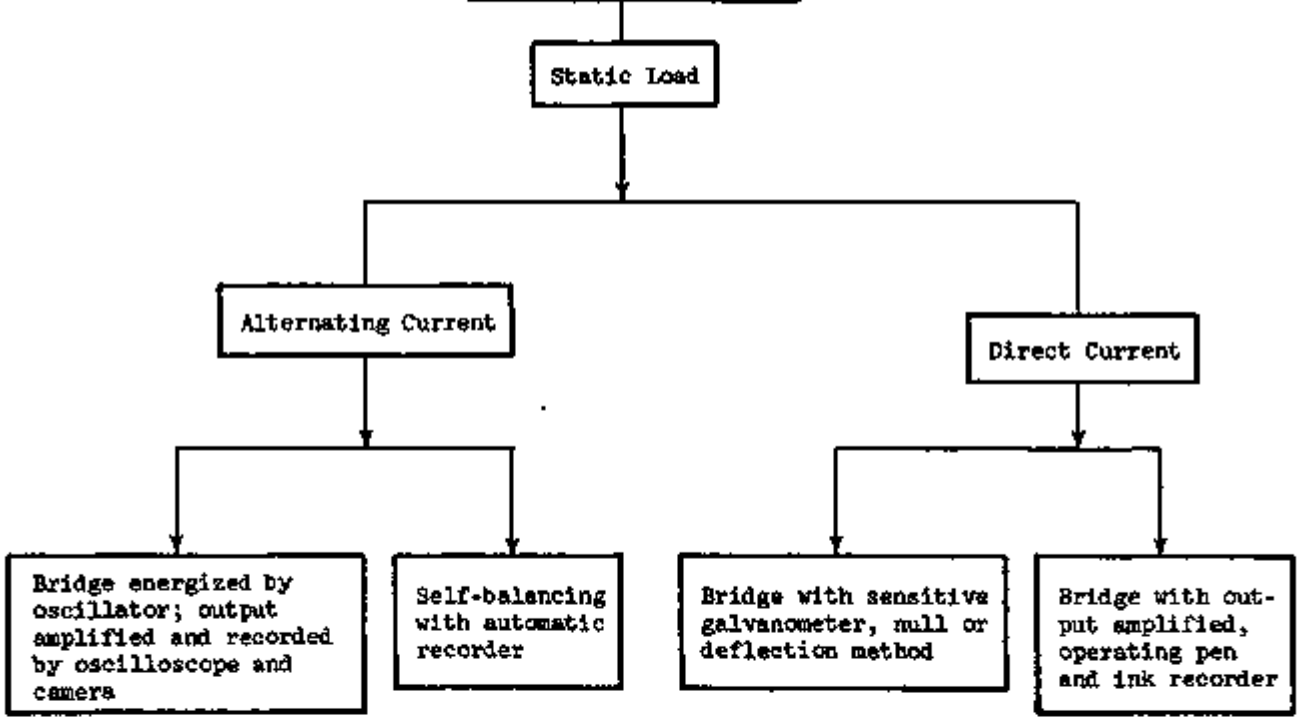

Strain gauges are normally connected to wheatstone bridge circuits to give direct readings of quantities otherwise not directly obtainable from a single gauge. It is also possible by different arrangements of the gauges to avoid certain unwanted strain effects.

(i) For tension stress: Figure 27 shows a back-to-back arrangement of gauges which is particularly useful in eliminating bonding stresses in thin sheets under direct stress. A dummy gauge must be employed and only one arm of the bridge must be active.

(ii) For bending stress: Figure 28 shows a similar arrangement for eliminating the axial stress in bending. In this case, one gauge acts as the dummy for the other and two arms of the bridge are active, which doubles the sensitivity.

(f) Procedure--Static bending test: The apparatus shown in Fig. 25 will be used to impart fibrax (bending) stress on the specimens. One end of the specimens will be clamped in a holder and the other end attached to long rods extending outside of both the container (pot), and the crucible furnace. The bending apparatus, the container (pot), and solid NaOH pellets will be transferred to a dry box having absolute inert gas atmosphere. The container will be filled with NaOH pellets and bending apparatus mounted inside it. The top plug will be bolted to the flange of the container and firmly sealed. Thus, assembly of the test system in inert atmosphere will keep moisture and air away from hygroscopic NaOH. Finally, this assembly will be placed in a crucible furnace.

When the desired operating temperature in the crucible furnace has been reached, the shaft supporting the bending apparatus assembly will be pushed down to expose the specimens to fused NaOH. Dead weights will be placed on the rods extending outside of the furnace. Both load and sinking of the rod will be recorded. Knowing the cross-sectional area of the specimens at bending plane, maximum stress can be calculated. Deflection of the cantilever beam and strain can be calculated from sinking of the rod.

The preferred method of registering strain is to attach strain gauges to specimens, and monitor them with a recorder. The recorder is also expected to detect the onset of cracking from the sudden changes in strain. The time at which this occurs can be detected without the presence of the experimenter.

The cantilever bending experiment was chosen because it is the simplest design. It can transmit and confine maximum stresses at the specimen surfaces to the vicinity of the hinge. Both tensile stress and compressive stress are simultaneously imparted to the sample. Since only the tensile stresses are responsible for initiating SCC, it is obvious that the investigator can have a wide range of flexibility as to imparting the level of stress intensity and confining it to one particular

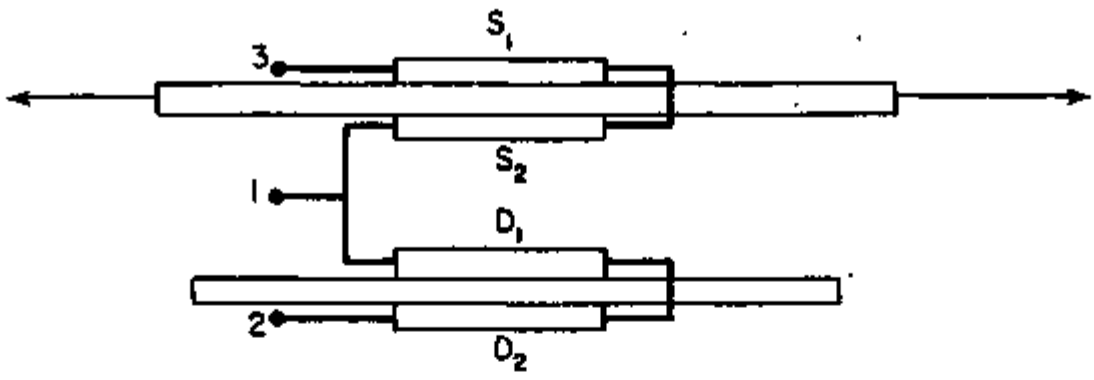

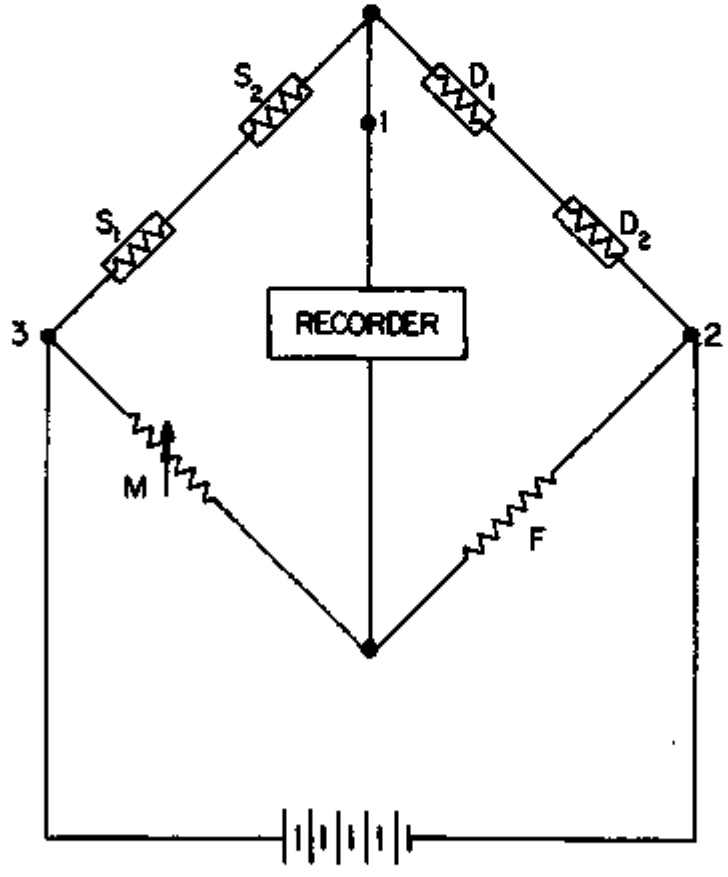

Fig. 27 - Arrangement of Gauges: Direct Stress

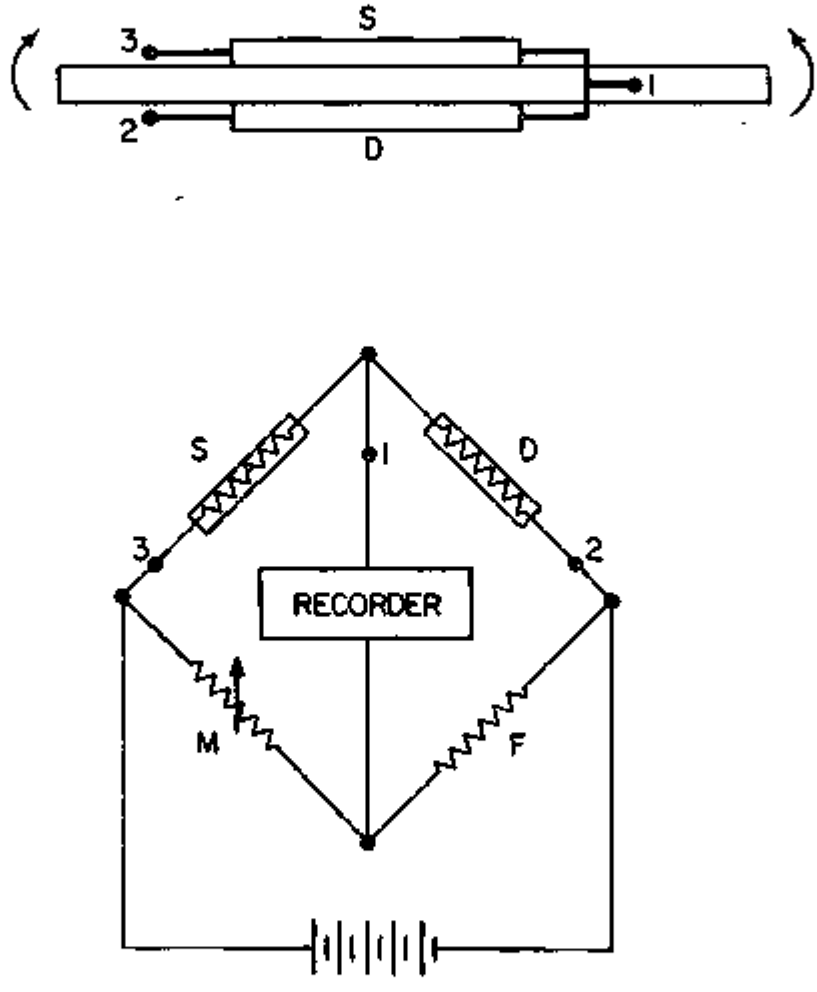

Fig. 28 - Arrangement of Gauges: Bending Stress

face of the specimen. Information can be obtained on the relative damages imparted to specimens at each particular stress level, e.g., the number of cracks introduced. Number of cracks can be verified with a high magnification optical microscope.

The level of stress necessary to initiate cracking will be easier to define as compared to establishing a critical level of stress for crack propagation. The onset of cracking can be determined by subjecting specimens through constant load or constant strain; constant load being the easier of the two. Thus, when the constant load approach is employed, the start of cracking can be detected by the sudden increase in stresses on the remaining (intact) metal. Further, cracking of the remainder metal will be accelerated by a combination of increased stress and stress concentration produced from the notch effect. For the constant strain approach, the initiation of cracking leads to some relaxation and resulting reduction of stress.

In the experimental setup described above the variables, such as load (stress), deflection (strain), bath temperature (fused NaOH), and environment above fused NaOH (inert gases), can be easily controlled.

Static tensile SCC test: The apparatus, assembly, and procedure will be similar to that described above. A difference between the two setups will be in design of the load rod. In the present case, a rod will be actuated to pull the specimen in tension instead of bending it. Another difference will be that the individual specimen will be exposed to isolated fused NaOH bath, i.e., one specimen to one container. This will enable the investigator to perform potentiometric measurements. In the bending test, where both compressive and tensile stresses exist, it is difficult to ascertain which stress is responsible for the changes in potential. The tensile test is a widely known standard type of test, and it is simple to perform.

Dynamic SCC test: The apparatus, assembly, and procedure will be similar to that described in the static bending test. In addition, a shaft mounted propeller will be used in the bath to set fused NaOH in dynamic motion against static specimens. The test is aimed at stimulating the actual conditions of reactor heat transfer system, where fused NaOH will be in motion with respect to the static boiler tubes.

Task 6 - The Straining Electrode and Transient Dissolution

A. Aims

In other work at OSU it has been shown that the straining electrode provides a good method for identifying those regions of electrochemical potential where SCC is most likely. The purpose of this task is to extend this understanding to caustic systems.

B. Results

None this Quarter.

Task 7 - Initiation and Propagation of Cracks

A. Aims

The aim of this work is to study initiation and propagation processes in single crystals of Fe-Cr-Ni alloys. Special attention will be paid to the crystallography of initiation on fracture processes. This work emphasizes metallurgical variables.

B. Results

None this Quarter.

Task 8 - Corrosion Processes in Crevices

A. Aims

The aim of this work is to define electrochemical processes in crevices associated with caustic environments. Crevice effects include accelerated corrosion as well as the formation of insoluble corrosion products which expand and exert substantial forces. Both of these processes can be very destructive.

B. Results

None this Quarter.

Task 9 - Dissolution at Grain Boundaries

A. Aims

Caustic SCC frequently occurs intergranularly and substantial intergranular attack is observed frequently when alloys are exposed to caustic environments. The purpose of this work is to define the amount and mechanism of intergranular corrosion and also that portion which is accelerated by stress.

B. Results

None this Quarter.

Task 10 - Local Dissolution Processes on Caustic Environments

A. Aims

The aim of this work is to investigate initiation processes using thin foils which can be exposed to the environment, stressed, and subsequently examined in the electron microscope.

B. Results

None this Quarter.

Task 11 - Metallurgical Structure

A. Aims

The susceptibility of many alloys to SCC can be drastically altered by changing the metallurgical structure. Such changes can be effected by cold work precipitation hardening, special heat treatments and changes in alloy composition to produce certain phases. This work will consider possibilities for applying these procedures for preventing SCC.

B. Results

None this Quarter.

Task 12 - Detailed Nature of the Passive Film

A. Aims

The aim of this task is to define the detailed aspects of chemistry and structure of the protective film on the surface of Fe-Cr-Ni alloys in caustic environments. This effect is important because all chemical reactions and stress corrosion cracking are related directly to the chemical or mechanical breakdown of these protective films.

B. Results

None this Quarter.

5.0 REFERENCES

1. H. D. Ongman, Nuclear Superheat Project, Final Report, G.E.A.P., 5087 (1965).

2. L. R. Scharfstein and W. D. Brindlay, Corrosion, 14 (1968) 588t.

3. D. V. Subrahmanyam in Quarterly Report No. COO-2018-11(Q-2), USAEC (1969).

4. C. T. Cron, J. H. Payer, and R. W. Staehle, Corrosion, 27 (1971)1.

5. K. G. Sheth in Quarterly Report No. COO-2018-8(Q-3), USAEC, (1969).

6. K. G. Sheth in Quarterly Report No. COO-2018-18(Q-5), USAEC, (1970).

7. R. N. O'Brien and P. Seto, J. Electrochem. Soc., 117 (1970), 32.

8. V. V. Batrakov, A. P. Pyankova, and Z. A. Iofa, Russ. J. Phys. Chem., 38 (1964), 733.

9. J. W. Chastain and R. W. Dayton, "Hydroxides as Moderator Coolants in Power Breeder Reactor," USAEC Report BMI 746, Battelle Memorial Institute (May 1952).

10. H. A. Pray and P. D. Miller, "The Mechanism of the Corrosion of Nickel in Molten Sodium Hydroxide," USAEC Report BMI-760, Battelle Memorial Institute, (July 1953).

11. C. M. Craighead, L. A. Smith, and R. I. Jaffee, "Screening Tests on Metals and Alloys in Contact with Sodium Hydroxide at 1000 and 1500°F," USAEC Report BMI-706, Battelle Memorial Institute, (Nov. 1951).

12. C. M. Craighead, L. A. Smith., E. C. Phillips, and R. E. Jaffee, "Continued Studies of Corrosion by Fused Caustic," USAEC Report AECD-3704, Battelle Memorial Institute, (Dec. 1952).

13. R. S. Peoples, P. D. Miller, and H. D. Hannan, "Reaction of Nickel in Molten Sodium Hydroxide," USAEC Report BMI-1401, Battelle Memorial Inst., (Sept. 1955).

14. G. P. Smith, "Corrosion of Materials in Fused Hydroxides," USAEC Report ORNL-2048, Oak Ridge National Laboratory, (March 1956).

15. A. D. Bogard, "The Solubility of Iron in Sodium Metal, Sodium-Sodium Oxide, and Sodium-Sodium Oxide-Sodium Hydroxide," Report NRL-4131, Naval Research Laboratory, (March 9, 1953).

16. D. R. Mosher and R. A. Lad, "Kinetic Study of Mass Transfer by Sodium Hydroxide in Nickel under Free-Convection Conditions," Report NACA-RM-E 53 K 24, Lewis Flight Propulsion Laboratory, Cleveland, (1953).

17. A. F. Forestieri and R. A. Lad, "Effectiveness of Inhibition for Mass Transfer and Corrosion in Sodium Hydroxide-Nickel Systems," Report NACA-RM-E 55 K 30, Lewis Flight Propulsion Lab., Cleveland (1956).

18. R. A. Lad and A. F. Forestieri, "The Use of Metallic Inhibitors for Eliminating Mass Transfer and Corrosion in Nickel and Nickel Alloy by Molten Sodium Hydroxide," Report NADA-RM-E 54 L 13, Lewis Flight Propulsion Lab., Cleveland (1954).

19. A. F. Forestieri and V. Zelenny, "Static Crucible Investigation of Corrosion and Mass Transfer of Nickel in Molten Sodium Hydroxide with Various Additives," Report NACA-RM-E 53 F 12, Lewis Flight Propulsion Lab., Cleveland, (Sept. 1953).

20. E. M. Simons, N. E. Miller, J. H. Stang, and C. V. Weaver, "Corrosion and Components Studied on Systems Containing Fused NaOH," USAEC Report BMI-1118, Battelle Memorial Institute, (July 1956).

21. A. F. Forestieri, "Effects of Additives on Corrosion and Mass Transfer in Sodium Hydroxide-Nickel Systems under Free-Convection Conditions," Report NACA-RM-E 54 E 19, Lewis Flight Propulsion Laboratory, Cleveland, (May 1954).

22. C. E. May, "Correlation between Hydrogen Pressure and the Protective Action of Additives in Molten NaOH-Ni System," Report NACA-RM-E 55 L 01, Lewis Flight Propulsion Laboratory, Cleveland, (Feb. 1956).

23. C. E. May, "Inhibition of Mass Transfer in Molten Sodium Hydroxide-Nickel System by Addition of Chromite," Report NACA-RM-E 55 L 02, Lewis Flight Propulsion Lab., Cleveland, (Feb. 1956).

24. D. D. Williams and R. R. Miller, "Part II, High Temperature Reaction of Sodium Hydroxide," Report WADC-TR-54-185, Naval Research Lab., (Feb. 1955).

25. R. S. Peoples, P. D. Miller and H. D. Hannan, "Reaction of Nickel in Molten Sodium Hydroxide," USAEC, Report BMI-979, Battelle Memorial Institute (Feb. 1955).

26. V. E. Baum, Z. Electrochem., 27 (1921).

27. J. N. Agar and F. P. Bowden, "The Kinetics of Electrode Reaction I and II," Proc. Royal Soc. (London), A169 (1938) 220.

28. Lux, Naturwiss, 18 (1949) 43.

29. Lux, Z. Elektrochem., 53 (1949) 43.

30. I. D. Dirmeik, "Anodic Passivation of Metals in Fused Salt Electrolyte, Corrosion, 25 (1969) 181.

31. K. H. Stern and J. K. Carlton, Electrode Potentials in Fused System, I. Sodium Hydroxide," J. Phys. Chem., 58 (1954) 965.

Investigator ..... Date .....

Supervisor ..... Date 18 March 1971

For The Ohio State University Research Foundation

Executive Director Robert C. Stephenson Date 24 March 1971